NASA/TP—2009–215687

Predicting the Size of Sunspot Cycle 24 on the Basis of Single- and Bi-Variate Geomagnetic Precursor Methods

Robert M. Wilson and David H. Hathaway
Marshall Space Flight Center, Marshall Space Flight Center, Alabama

February 2009

The NASA STI Program…in Profile

Since its founding, NASA has been dedicated to the advancement of aeronautics and space science. The NASA Scientific and Technical Information (STI) Program Office plays a key part in helping NASA maintain this important role.

The NASA STI program operates under the auspices of the Agency Chief Information Officer. It collects, organizes, provides for archiving, and disseminates NASA's STI. The NASA STI program provides access to the NASA Aeronautics and Space Database and its public interface, the NASA Technical Report Server, thus providing one of the largest collections of aeronautical and space science STI in the world. Results are published in both non-NASA channels and by NASA in the NASA STI Report Series, which includes the following report types:

- TECHNICAL PUBLICATION. Reports of completed research or a major significant phase of research that present the results of NASA programs and include extensive data or theoretical analysis. Includes compilations of significant scientific and technical data and information deemed to be of continuing reference value. NASA's counterpart of peer-reviewed formal professional papers but has less stringent limitations on manuscript length and extent of graphic presentations.

- TECHNICAL MEMORANDUM. Scientific and technical findings that are preliminary or of specialized interest, e.g., quick release reports, working papers, and bibliographies that contain minimal annotation. Does not contain extensive analysis.

- CONTRACTOR REPORT. Scientific and technical findings by NASA-sponsored contractors and grantees.

- CONFERENCE PUBLICATION. Collected papers from scientific and technical conferences, symposia, seminars, or other meetings sponsored or cosponsored by NASA.

- SPECIAL PUBLICATION. Scientific, technical, or historical information from NASA programs, projects, and missions, often concerned with subjects having substantial public interest.

- TECHNICAL TRANSLATION. English-language translations of foreign scientific and technical material pertinent to NASA's mission.

Specialized services also include creating custom thesauri, building customized databases, and organizing and publishing research results.

For more information about the NASA STI program, see the following:

- Access the NASA STI program home page at <http://www.sti.nasa.gov>

- E-mail your question via the Internet to <help@sti.nasa.gov>

- Fax your question to the NASA STI Help Desk at 443–757–5803

- Phone the NASA STI Help Desk at 443–757–5802

- Write to:
  NASA STI Help Desk
  NASA Center for AeroSpace Information
  7115 Standard Drive
  Hanover, MD 21076–1320

NASA/TP—2009–215687

Predicting the Size of Sunspot Cycle 24 on the Basis of Single- and Bi-Variate Geomagnetic Precursor Methods

Robert M. Wilson and David H. Hathaway
Marshall Space Flight Center, Marshall Space Flight Center, Alabama

National Aeronautics and
Space Administration

Marshall Space Flight Center • MSFC, Alabama 35812

February 2009

Available from:

NASA Center for AeroSpace Information
7115 Standard Drive
Hanover, MD 21076–1320
443–757–5802

This report is also available in electronic form at
<https://www2.sti.nasa.gov>

TABLE OF CONTENTS

LIST OF FIGURES

LIST OF TABLES

NOMENCLATURE

12-mma	12-mo moving average
#	post-$E(RM)$ value, unless otherwise stated
*	value in the vicinity of cycle minimum, unless otherwise stated
a	y-axis intercept
AA	12-mma of aa
aa	daily or monthly mean of the aa geomagnetic index
$<aa(-36)>$	average value of aa within 36 mo prior to $E(Rm)$
$AA(I)$	12-mma of $aa(I)$
$aa(I)$	monthly value of the $aa(I)$ geomagnetic index
$<aa(I)(-36))>$	average value of $aa(I)$ within 36 mo prior to $E(Rm)$
$AA(I)M$	maximum value of $AA(I)$
$AA(I)m$	minimum value of $AA(I)$
$AA(I)M(lp)$	late-peak value of $AA(I)M$
AAM	maximum value of AA
$AAM(lp)$	late-peak value of AAM
AAm	minimum value of AA
ad	average deviation
AP	12-mma of ap
ap	daily or monthly mean of the ap geomagnetic index
$<ap(-36>)$	average value of ap within 36 mo prior to $E(Rm)$
APM	maximum value of AP
APm	minimum value of AP
$APM(lp)$	late-peak value of APM
b	slope
cl	confidence level
DI	12-mma of di

NOMENCLATURE (Continued)

di	disturbance index; i.e., the number of days in a month when *ap* ≥25 nT
<*di*(–36)>	average value of *di* within 36 mo prior to *E*(*Rm*)
di(sum)	sum of *di* over a sunspot cycle
DIM	maximum value of *DI*
DIm	minimum value of *DI*
DIM(*lp*)	late-peak value of *DIM*
E	epoch of occurrence
lp	late-cycle peaks
m	minimum parametric value
n	sunspot cycle number; the number of cycles in the sample
R	12-mma of monthly mean sunspot number
r	coefficient of correlation
r^2	coefficient of determination
RM	12-mma of the maximum value of *R*
Rm	12-mma of the minimum value of *R*
RM(24)	predicted maximum amplitude for cycle 24
RM(sum)	sum of *RM* for two consecutive sunspot cycles
sd	standard deviation
se	standard error of estimate
t	elapsed time in months from *E*(*Rm*)
t′	elapsed time in months from the following cycle's *E*(*Rm*)
V	12-mma of the monthly mean solar wind velocity in kms^{-1}
VM	12-mma of the maximum value of *V*
Vm	12-mma of the minimum value of *V*
Vm′	12-mma of the minimum value of *V* during the decline of cycle 23
x	independent variable
y	inferred regression equation using entire sample
y^*	inferred regression equation ignoring a statistical outlier

TECHNICAL PUBLICATION

PREDICTING THE SIZE OF SUNSPOT CYCLE 24 ON THE BASIS OF SINGLE- AND BI-VARIATE GEOMAGNETIC PRECURSOR METHODS

1. INTRODUCTION

Attempts to accurately predict the strength of a sunspot cycle in advance, based on a variety of methods and statistical techniques, have met with only limited success.[1] For example, cycle 23, the current ongoing sunspot cycle, had a wide range of predictions[2–5] for its size, from about 80 to 210. It is now known to have measured 120.8, having peaked in April 2000. Even those based on dynamo-related models have not always faired well. For example, using the strength of the polar fields near sunspot minimum, Schatten et al.[6] estimated the size of cycle 21 (164.5) to be about 140 ± 20, a fairly good estimate, while Schatten and Hedin[7] estimated the size of cycle 22 (158.5) to be about 109 ± 20 and Schatten and Pesnell[8] estimated the size of cycle 23 (120.8) to be about 170 ± 25, both rather poor estimates. Of the various methods and techniques used to predict the size of an upcoming or just starting sunspot cycle, those based on precursor geomagnetic information usually have provided the best predictions.[1,9]

In this Technical Publication (TP), both single- and bi-variate fits, based on precursor geomagnetic indices in various combinations including with sunspot minimum amplitude, are examined to estimate the expected size of cycle 24, the next sunspot cycle.

2. RESULTS

2.1 Cycle 23 Behavioral Characteristics

Figure 1 displays the general behavioral characteristics of cycle 23 through April 2008. Figure 1(a) shows the variation of the 12-mo moving average (12-mma) of monthly mean sunspot number (*R*). Its minimum (*Rm*) occurred in May 1996 (*E*(*Rm*)) and measured 8.0. While minimum amplitude often is used to establish the onset of a sunspot cycle, a better determination is one based on several parameters, such as the number of spotless days, the ratio of the number of new cycle to old cycle spots, etc.[10,11] For cycle 23, this would indicate a slightly later-occurring minimum, perhaps, about August–October 1996. However, for the purpose of this TP, because of its simplicity, it is convenient to use the occurrence of *Rm* as representing the onset of a sunspot cycle.

Cycle 23's maximum amplitude (*RM*, 120.8) occurred in April 2000 at $t=47$ mo, where *t* is the elapsed time in months from *E*(*Rm*), with a slightly smaller secondary peak (115.5) having occurred in November 2001 at $t=66$ mo. Hence, on the basis of the 12-mma of *R*, cycle 23 can be described as being double-peaked, as many previous sunspot cycles have been so described.

April 2008, presuming it does not represent *E*(*Rm*) for cycle 24 since March and April 2008 have 12-mma values of *R* that both measure 3.3, marks the 144th month since cycle 23's *E*(*Rm*), making cycle 23 the longest running sunspot cycle since cycle 9 (149 mo) and the 5th longest running cycle in the span of cycles 1–23. On the basis of the most reliably known sunspot cycles 12–22, longer period cycles have minimum-to-minimum lengths, or periods, equal to about 139 ± 7 mo (the 90% prediction interval), indicating that *E*(*Rm*) for cycle 24 should be most imminent;[12,13] i.e., there is only about a 5% chance that cycle 23 will have a period equal to or longer than 147 mo, indicating *E*(*Rm*) for cycle 24 probably before July 2008; 12-mma values of R, also called 'smoothed monthly mean sunspot numbers,' are readily available at <ftp://ftp.ngdc.noaa.gov/STP/>.[14]

Figure 1(b) depicts the variation of the 12-mma of the *AA* and *AA*(*I*) geomagnetic indices, where the *AA* index is the corrected *AA* index; i.e., values prior to 1957 are increased by 3 nT to compensate for repositioning of the magnetometers used in determining the value of the *AA* index,[15,16] and *AA*(*I*) is the interplanetary component of the *AA* index, attributed to the occurrence of high-speed streams in the solar wind due to the presence of coronal holes.[17–20] The *AA*(*I*) index, which is the residual of the *AA* index having removed the solar cycle-related component, is found to mimic the overall *AA* index. Both *AA* and *AA*(*I*) indices had minimum values (15.8 and 8.3, respectively) in October 1997 at $t=17$ mo and maximum values (38.0 and 28.9, respectively) in August 2003 at $t=87$ mo, with smaller secondary maximums (25.3 and 17.6, respectively) about April 2005 at $t=107$ mo. The lowest recent values are 14.9 for the *AA* index and 8.2 for the *AA*(*I*) index in July 2007 at $t=134$ mo. Because minimum values almost always have followed *E*(*Rm*), the lone exception being cycle 14, *AA* and *AA*(*I*) current values are expected to slowly decrease in 2008 to values below the July 2007 minimum values unless, of course, cycle 24 is kindred to cycle 14.

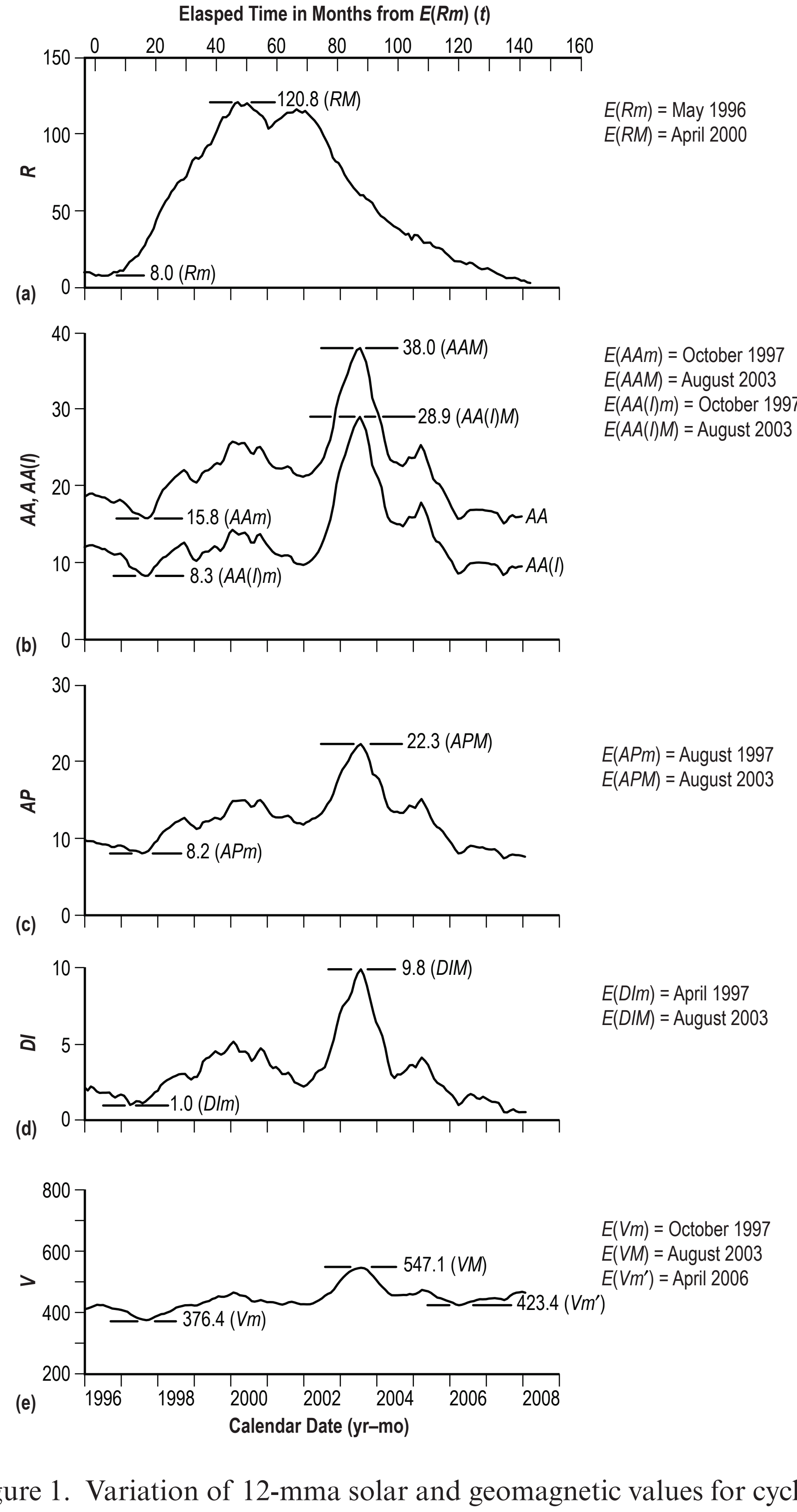

Figure 1. Variation of 12-mma solar and geomagnetic values for cycle 23, January 1996 through April 2008.

Figure 1(c) shows the variation of the 12-mma of the *AP* index and its behavior is found to strongly mimic the behaviors of the *AA* and *AA*(*I*) indices, having a minimum of 8.2 in October 1997, primary maximum of 22.3 in August 2003, and a smaller secondary maximum of 15.1 in April 2005. The lowest recent value is 7.4 in July 2007, although the overall recent trend appears downward, so that a lower *APm* seems likely in 2008–2009.

Figure 1(d) displays the variation of the 12-mma of the disturbance index (*DI*), which is deduced from the *AP* index. In particular, the disturbance index is the number of days when the daily *ap* index is ≥25 nT, summed over an entire month. The *DI* bears a strong resemblance, not only to the *AP* index, but also to the *AA* and *AA*(*I*) indices as well, having a minimum of 1.0 slightly earlier in April 1997, a primary maximum of 9.8 in August 2003, and a smaller secondary maximum of 4.1 in April 2005. Values of 0.5 have been recorded in July–August 2007 and December 2007–March 2008, this being the lowest value observed to date. A slightly lower *DIm* might be expected, especially, if lower *AA*, *AA*(*I*) and *AP* indices occur. Otherwise, 0.5 will be the value for *DIm* for cycle 24. (The *DI* index has proven important for predicting the later-occurring *RM* using different methodologies.[1,21–23])

Figure 1(e) depicts the variation of the 12-mma of the solar wind velocity in kms^{-1} (*V*). It too is found to strongly mimic the behavior of *AA*, *AA*(*I*); *AP*; and *DI*. Indeed, linear correlation analysis reveals close correlation, especially between *V* and *AA*(*I*), having a correlation coefficient of $r = 0.931$ for the interval January 1996–December 2006.[24] For the interval 1964–2006, a slightly weaker correlation is observed, due to poorer coverage in the determination of solar wind speeds in earlier years. Here, solar wind speeds are based on the average minimum and maximum daily solar wind speeds for each month, weighted according to the number of hours of daily observation, using the Omni-merged 1-hr, 1 AU interplanetary data available at <http://cdaweb.gsfc.nasa.gov>.[25] A minimum solar wind speed of 376.4 kms^{-1} was observed in October 1997, a primary maximum of 547.1 kms^{-1} in August 2003, and a smaller secondary maximum of 472.3 kms^{-1} in April 2005. The lowest *V* since the secondary maximum measures 423.4 kms^{-1} in April 2006. Higher *V* has been seen since the April 2006 minimum, in contrast to the apparent movements of the *AA*, *AA*(*I*); *AP*; and *DI* indices, which seem to be moving either flatly or slightly downward. However, because of the inferred strong relationship existing between solar wind speed and the geomagnetic indices, it seems likely that a lower solar wind speed minimum (*Vm*) will be seen sometime in 2008–2009.

2.2 Minimum and Maximum Values for Selected Solar and Geomagnetic Parameters for Cycles 11–24

Table 1 gives minimum and maximum amplitudes for *R*, *AA*, *AA*(*I*), *AP*, and *DI* for cycles 11–24 (tentative values for cycle 24), as well as averages for the 36 mo prior to *E*(*Rm*) for *aa*, *aa*(*I*), *ap*, and *di*, and it also gives the sum of *di* over an entire cycle (*E*(*Rm*) cycle *n* to *E*(*Rm*) cycle $n+1$). For the most reliably determined cycles 12–23, the ±1-*sd* intervals about the mean for *Rm*, *AAm*, and *AA*(*I*)*m* are 6.1 ± 3.8, 14.6 ± 3.6, and 7.0 ± 3.4, respectively, and the lowest observed values to date for cycle 24 for these parameters are 3.3, 14.9, and 8.2, respectively, all lying well within these intervals. For *RM*, the ±1-*sd* interval is 119.7 ± 41.9. For *AAM* and *AA*(*I*)*M*, using cycles 11–22 since the maximum value of these parameters might be related to the following cycle's *RM*, the ±1-*sd* intervals are 30.2 ± 4.2 and 20.9 ± 3.6, respectively. The maximum values (38.0 and 28.9, respectively) in cycle 23 are well outside-high with respect to these intervals, being the largest ever recorded. For the averages <*aa*(–36)> and

Table 1. Selected solar and geomagnetic parametric values for cycles 11–24.

Cycle	*Rm*	*RM*	*AAm*	*AAM*	*AA*(*I*)*m*	*AA*(*I*)*M*	*APm*	*APM*	*DIm*	*DIM*	<*aa*(–36)>	<*aa*(I)(–36)>	<*ap*(–36)>	<*di*(–36)>	*di*(sum)
11	5.2	140.5	–	27.4	–	17.1	–	–	–	–	–	–	–	–	–
12	2.2	74.6	9.7	26.8[@]	3.2	17.8[@]	–	–	–	–	11.5	4.8	–	–	–
13	5.0	87.9	13.6	27.1[&]	7.0	17.4[&]	–	–	–	–	17.3	10.6	–	–	–
14	2.6	64.2	8.9	22.2	2.4	15.4	–	–	–	–	11.9	5.1	–	–	–
15	1.5	105.4	11.2	27.4	4.8	17.5	–	–	–	–	15.7	9.2	–	–	–
16	5.6	78.1	12.4	32.0	5.1	23.6	–	–	–	–	19.3	12.0	–	–	–
17	3.4	119.2	16.2	29.5	8.3[%]	22.7	7.2	18.0	0.7	7.5	21.2	14.1	–	–	488
18	7.7	151.8	19.3	34.7	11.5	26.2	10.2	25.0	1.9	11.7	27.1	19.4	15.8	5.6	689
19	3.4	201.3	19.9	32.7	12.8	21.5	10.8	23.6	1.8	8.6	28.7	20.9	19.2	8.1	618
20	9.6	110.6	13.8	30.8	6.7*	23.0	7.7	19.8	0.8	8.3	20.5	12.9	12.0	3.3	497
21	12.2	164.5	17.2[#]	34.6	3.6[#]	24.8	10.4[#]	23.2	1.8	9.5	26.2	18.7	16.2	6.1	588
22	12.3	158.5	17.5	36.7	10.4	23.7	10.0	25.0	1.4	10.2	25.0	17.8	15.6	4.9	613
23	8.0	120.8	15.8	38.0	8.3	28.9	8.2	22.3	1.0	9.8	24.4	16.9	14.4	5.2	454
24[$]	3.3	–	<14.9	–	<8.2	–	<7.4	–	<0.5	–	17.5	10.5	9.4	1.6	–

Notes: [@] indicates that the value occurred prior to *E*(*RM*); the highest value post *E*(*RM*) measured 23.7 for *AAM* and 16.3 for *AA*(*I*)*M*.
[&] indicates that the value occurred prior to *E*(*RM*); the highest value post *E*(*RM*) measured 23.9 for *AAM* and 13.9 for *AA*(*I*)*M*.
[%] indicates that the value occurred near *E*(*RM*); the lowest value in the vicinity of *E*(*Rm*) measured 9.6.
* indicates that the value occurred post *E*(*RM*); the lowest value prior to *E*(*RM*) measured 6.8.
[#] indicates that the values occurred post *E*(*RM*); the lowest value prior to *E*(*RM*) measured 19.6 for *AAm*, 12.6 for *AA*(*I*)*m* and 10.8 for *APm*.
[$] indicates that the values for cycle 24 are tentative, presuming *E*(*Rm*) in March 2008.

Legend:
Rm = minimum value of the 12-mma of the monthly mean *R*.
RM = maximum value of the 12-mma of the monthly mean *R*.
AAm = minimum value of the 12-mma of the monthly mean *aa* index.
AAM = maximum value of the 12-mma of the monthly mean *aa* index.
AA(*I*)*m* = minimum value of the 12-mma of the monthly mean *aa*(*I*) index.
AA(*I*)*M* = maximum value of the 12-mma of the monthly mean *aa*(*I*) index.
APm = minimum value of the 12-mma of the monthly mean *ap* index.
APM = maximum value of the 12-mma of the monthly mean *ap* index.
DIm = minimum value of the 12-mma of the monthly mean *DI* index.
DIM = maximum value of the 12-mma of the monthly mean *DI* index.
<*aa*(–36)> = average value of the *aa* index from 36 mo prior to *E*(*Rm*) to *E*(*Rm*).
<*aa*(*I*)(–36)> = average value of *aa*(*I*) from 36 mo prior to *E*(*Rm*) to *E*(*Rm*).
<*ap*(–36)> = average value of the *ap* index from 36 mo prior to *E*(*Rm*).
<*di*(–36)> = average value of *di* from 36 mo prior to *E*(*Rm*) to *E*(*Rm*).
di(sum) = sum of *di* for a particular cycle, from *E*(*Rm*) to succeeding cycle *E*(*Rm*).
E(*Rm*) = epoch of sunspot minimum amplitude.
E(*RM*) = epoch of sunspot maximum amplitude.

<*aa*(*I*)(–36)>, the ±1-*sd* intervals about the means for cycles 12–23 are 20.7±5.8 and 13.5±5.4, respectively. The values for cycle 24, presuming *E*(*Rm*) in March 2008, are 17.5 and 10.5, respectively, well within the interval ranges.

For *APm* and *DIm*, the ±1-*sd* intervals about the means using cycles 17–23 (*AP* and, consequently, *DI* are directly known only from 1932, or from cycle 17 onwards) are 9.2±1.5 and 1.3± 0.5, respectively. The lowest observed values to date for cycle 24 are 7.4 and 0.5, respectively, both values outside-low as compared to their respective ±1-*sd* intervals about the means. For *APM* and *DIM*, the ±1-*sd* intervals about the means for cycles 17–22 are 22.4±2.9 and 9.3±1.5, respectively. The maximum values (22.3 and 9.8, respectively) in cycle 23 lie within these respective intervals. For <*ap*(–36)> and <*di*(–36)>, the ±1-*sd* intervals about the means for cycles 18–22 are 15.5±2.4 and 5.5±1.6, respectively. The values for cycle 24, presuming *E*(*Rm*) in March 2008, are 9.4 and 1.6, respectively, both well outside-low their respective interval ranges. For *di*(sum), the ±1-*sd* interval about the mean for cycles 17–22 is 582.2 ± 77.2. The *di*(sum) for cycle 23 is 454, which also is outside-low as compared to the ±1-*sd* interval about the mean.

It is important to note that some of the parametric values occur oddly with respect to *E*(*Rm*) and *E*(*RM*). For example, cycles 12 and 13 had *AAM* and *AA*(*I*)*M* prior to their respective *E*(*RM*) dates, in contrast to all other cycles. For these cycles, alternate maximum values can be determined post-*E*(*RM*) as indicated in the note below table 1. Similarly, for cycle 21, its *AAm*, *AA*(*I*)*m*, and *APm* values occurred in 1980, near *E*(*RM*), in stark contrast to most of the other cycles, although again, alternate minimum values can be determined in the vicinity of cycle minimum for cycle 21, as so described in the note below table 1. Likewise, an alternate minimum value in the vicinity of cycle minimum can be determined for *AA*(*I*)*m* for cycles 17 and 20, as so described in notes below table 1. The values for cycle 24 are tentative and probably will fall below those given in table 1, especially for *AAm*, *AA*(*I*)*m*, *APm*, and *DIm*. However, *Rm* likely will remain 3.3, given the recent surge in activity in November 2008, which should increase 12-mma values of *R* for May 2008. (A possible maximum in the 12-mma of the number of spotless days occurred in March 2008 and a minimum in the 12-mma of the number of spot groups occurred in February 2008, both factors indicating the imminent onset of cycle 24's *E*(*Rm*), since they usually occur within a few months either side of *E*(*Rm*).)

Table 2 gives epochs of minimum and maximum for *R*, *AA*, *AA*(*I*), *AP*, and *DI* for cycles 11–24 (month and year), presuming sunspot minimum for cycle 24 about March 2008. Alternate epochs are noted in notes below table 2 for certain parameters (*AAm*, *AA*(*I*)*m*, and *APm* for cycle 21, *AA*(*I*)*m* for cycles 17 and 20, and *AAM* and *AA*(*I*)*M* for cycles 12 and 13).

Table 2. Epochs of minimum and maximum solar and geomagnetic parametric values for cycles 11–24.

Cycle	*E*(*Rm*)	*E*(*RM*)	*E*(*AAm*)	*E*(*AAM*)	*E*(*AA*(*I*)*m*)	*E*(*AA*(*I*)*M*)	*E*(*APm*)	*E*(*APM*)	*E*(*DIm*)	*E*(*DIM*)
11	03 1867	08 1870	–	01 1873	–	01 1873	–	–	–	–
12	12 1878	12 1883	01 1879	09 1882*	09 1879	09 1882*	–	–	–	–
13	03 1890	01 1894	07 1890	07 1892#	07 1890	07 1892#	–	–	–	–
14	01 1902	02 1906	09 1901	01 1911	12 1900	01 1911	–	–	–	–
15	08 1913	08 1917	09 1913	12 1918	09 1913	12 1918	–	–	–	–
16	08 1923	04 1928	10 1924	05 1930	10 1924	06 1930	–	–	–	–
17	09 1933	04 1937	06 1934	10 1943	02 1937%	10 1943	06 1934	10 1939	06 1934	10 1943
18	02 1944	05 1947	04 1945	12 1951	07 1945	01 1952	12 1944	12 1951	12 1944	11 1951
19	04 1954	03 1958	04 1955	06 1960	05 1955	09 1960	05 1955	06 1960	10 1954	05 1960
20	10 1964	11 1968	06 1965	09 1974	12 1969@	09 1974	05 1965	08 1974	06 1965	08 1974
21	06 1976	12 1979	04 1980$	12 1982	04 1980$	12 1982	04 1980&	11 1982	01 1977	11 1982
22	09 1986	07 1989	01 1987	09 1991	01 1987	09 1991	01 1987	09 1991	12 1986	09 1991
23	05 1996	04 2000	10 1997	08 2003	10 1997	08 2003	08 1997	08 2003	04 1997	08 2003
24	(03 2008)	–	(07 2007)	–	(07 2007)	–	(07 2007)	–	(02 2008)	–

Notes: * = The highest *AAM* and *AA*(*I*)*M* post *E*(*RM*) occurred 08 1886 and measured 23.7 and 16.3, respectively.
= The highest *AAM* and *AA*(*I*)*M* post *E*(*RM*) occurred 06 1894 and measured 23.9 and 13.9, respectively.
$ = The lowest *AAm* and *AA*(*I*)*m* in the vicinity of *E*(*Rm*) occurred 01 1977 and measured 19.6 and 12.6, respectively.
& = The lowest *APm* in the vicinity of *E*(*Rm*) occurred 12 1976 and measured 10.8.
% = The lowest *AA*(*I*)*m* in the vicinity of *E*(*Rm*) occured 06 1934 and measured 9.6.
@ = The lowest *AA*(*I*)*m* in the vicinity of *E*(*Rm*) occurred 05 1965 and measured 6.8.
Dates in parentheses are tentative, the dates of lowest value to date.

Table 3 gives the elapsed time in months of the epochs of minimum and maximum of the geomagnetic parameters relative to *E*(*Rm*) for cycles 11–24, where *t* is the elapsed time in months relative to cycle *n*'s *E*(*Rm*), and *t′* is the elapsed time in months relative to cycle $n+1$'s *E*(*Rm*) for the epochs of maximum amplitude. For *E*(*AAm*), on average, it usually follows *E*(*Rm*) by ≈7 mo, ranging from –4 mo (cycle 14) to 17 mo (cycle 23). Concerning cycle 14, its *t* could actually be longer, because the same *AAm* value (8.9) was seen at *t* = –5, –8, and –13 mo. For this TP, the last multiply-occurring value in time has been used to mark the epochs of minimum and maximum. If no smaller *AAm* occurs for cycle 24 (14.9), then *t* for cycle 24 will be at least –8 mo, which is unlike all other cycles except cycle 14.

Table 3. Elapsed time in months from *E*(*Rm*) for epochs of minimum and maximum geomagnetic parametric values for cycles 11–24.

	t								*t′*			
Cycle	***E*(*AAm*)**	***E*(*AA*(*I*)*m***	***E*(*APm*)**	***E*(*DIm*)**	***E*(*AAM*)**	***E*(*AA*(*I*)*M***	***E*(*APM*)**	***E*(*DIM*)**	***E*(*AAM*)**	***E*(*AA*(*I*)*M*)**	**(*E*(*APM*)**	***E*(*DIM*)**
11	–	–	–	–	70	70	–	–	–71	–71	–	–
12	1	9	–	–	92	92	–	–	–43	–43	–	–
13	4	4	–	–	51	51	–	–	–91	–91	–	–
14	–4	–13	–	–	107	107	–	–	–31	–31	–	–
15	1	1	–	–	64	64	–	–	–56	–56	–	–
16	14	14	–	–	81	82	–	–	–40	–39	–	–
17	9	9	9	9	121	121	73	121	–4	–4	–52	–4
18	14	17	10	10	94	95	94	93	–28	–27	–28	–29
19	12	13	13	6	74	77	74	73	–52	–49	–52	–53
20	8	7	7	8	119	119	118	118	–21	–21	–22	–22
21	7	7	6	7	78	78	77	77	–45	–45	–46	–46
22	4	4	4	3	60	60	60	60	–56	–56	–56	–56
23	17	17	15	11	87	87	87	87	(–55)	(–55)	(–55)	(–55)
24	(–8)	(–8)	(–8)	(0)	–	–	–	–	–	–	–	–

Notes: Minimum values used are those in the vicinity of *E*(*Rm*).
Maximum values are those post *E*(*RM*).
Positive values mean that the values occurred after *E*(*Rm*).
Negative values mean that the values occurred before *E*(*Rm*).
t means epochs relative to *E*(*Rm*) for cycle *n*.
t′ means epochs relative to *E*(*Rm*) for cycle $n+1$.
Values in parentheses are tentative, presuming *E*(*Rm*) for cycle 24 in March 2008 and that no lower minimum values will be seen.

Similarly, for *E*(*AA*(*I*)*m*), on average, it follows *E*(*Rm*) by ≈7 mo, ranging from –13 mo (cycle 14) to 17 mo (cycles 18 and 23). If no smaller *AA*(*I*)*m* occurs for cycle 24 (8.2), then *t* for cycle 24 will be at least –8 mo, again, unlike any of the other cycles except cycle 14.

E(*APm*) and *E*(*DIm*), on average, follow *E*(*Rm*) by about 9 and 8 mo, respectively, ranging from 4 mo (cycle 22) to 15 mo (cycle 23) and from 3 mo (cycle 22) to 11 mo (cycle 23), respectively. If no smaller *APm* and *DIm* occur, then *t* for cycle 24 (7.4 and 0.5, respectively) will be at least –8 and zero months, respectively, both values seemingly far too early with respect to what previous cycles have shown. Hence, it seems that smaller values of the geomagnetic parameters still lie ahead for cycle 24 unless, of course, cycle 24 proves to be kindred to cycle 14.

E(*AAM*) and *E*(*AA*(*I*)*M*), on average, follow *E*(*Rm*) by about 84 and 85 mo, respectively, ranging from 51 mo (cycle 13) to 121 mo (cycle 17) for both parameters. For cycle 23, its *E*(*AAM*) and *E*(*AA*(*I*)*M*) occurred at $t=87$ mo, essentially the same as the average *t* for cycles 11–22; so, cycle 23's *E*(*AAM*) and *E*(*AA*(*I*)*M*) relative to *E*(*Rm*) are not unusual. *E*(*APM*) and *E*(*DIM*), on average, follow *E*(*Rm*) by about 83 and 81 mo, respectively, ranging from 60 mo (cycle 22) to 118 mo (cycle 20) for *E*(*APM*) and ranging from 60 mo (cycle 22) to 121 mo (cycle 17) for *E*(*DIM*). Again, there appears nothing unusual about the occurrences of *E*(*APM*) and *E*(*DIM*) for cycle 23, both having $t=87$ mo, very close to the average *t*.

Relative to the following cycle's *E*(*Rm*), on average, *E*(*AAM*) and *E*(*AA*(*I*)*M*) precede the new cycle by about 45 and 44 mo, respectively, ranging from –4 mo (cycle 17) to –91 mo (cycle 13) for both parameters. For cycle 23, its *E*(*AAM*) and *E*(*AA*(*I*)*M*) will be at least –55 mo, well within the range, although slightly longer than the average of t' for cycles 11–22. If instead of using the primary maximums (38.0 and 28.9, respectively) one chose to use the later-occurring smaller secondary maximums (25.3 and 17.6, respectively), then t' would decrease to –35 mo, still well within the range, but now slightly shorter than the average t' for cycles 11–22.

E(*APM*) and *E*(*DIM*), on average, precede the new cycle by about 43 and 35 mo, respectively, ranging from –22 mo (cycle 20) to –56 mo (cycle 22) for the former parameter and from –4 mo (cycle 17) to –56 mo (cycle 22) for the latter parameter. For cycle 23, its *E*(*APM*) and *E*(*DIM*) will be at least –55 mo, within the ranges and of similar value to those of cycle 22. Instead, using the later-occurring smaller secondary maximums, cycle 23's t' decreases to –35 mo, still within the ranges, but now shorter than the averages and unlike any of the preceding cycles.

Figure 2 displays visually the cyclic variation of all the parameters identified in table 1, except the plotted minimum values are those occurring in the vicinity of *E*(*Rm*) and the plotted maximum values are those occurring post *E*(*RM*), as per the notes below table 1. Clearly, there is strong resemblance between the variation of *RM* as compared to the variations of the other parameters, except, perhaps, the variations of *AAM* and *AA*(*I*)*M* (figs. 2(g) and 2(h)), at least when including the last few cycles (21–23). Tentative minimum parametric values for cycle 24 (those in boxes) are situated either on the medians or more often below the medians.

Figure 3 shows the cyclic variations of selected alternate secondary late-cycle peaks (*lp*) for cycles 12–24, using *AAM*, *AA*(*I*)*M*, *APM*, and *DIM* geomagnetic indices. These peaks, usually occurring within the last few years of a sunspot cycle, are preferred by some investigators (L. Svalgaard, Private Communication, 2008) for predicting the size of the following cycle's maximum amplitude over using the true post-*E*(*RM*) maximums. However, it should be noted that often there are many peaks during the declining portion of a sunspot cycle, including within the last few years of a cycle, making it difficult to decide which peak is the 'best' peak to use for predicting later-occurring solar activity.

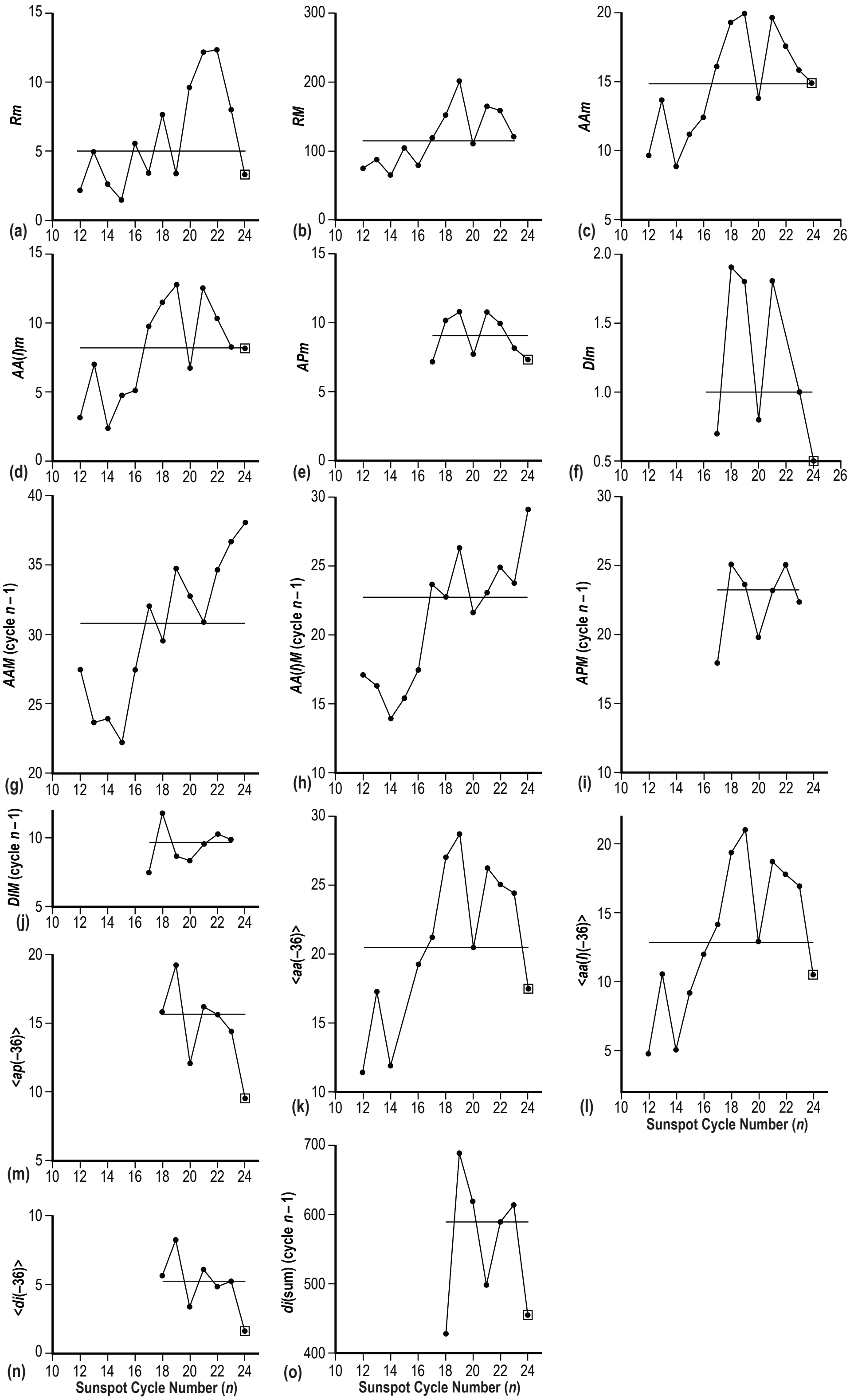

Figure 2. Cyclic variation of selected 12-mma solar and geomagnetic parametric values for cycles 11–24.

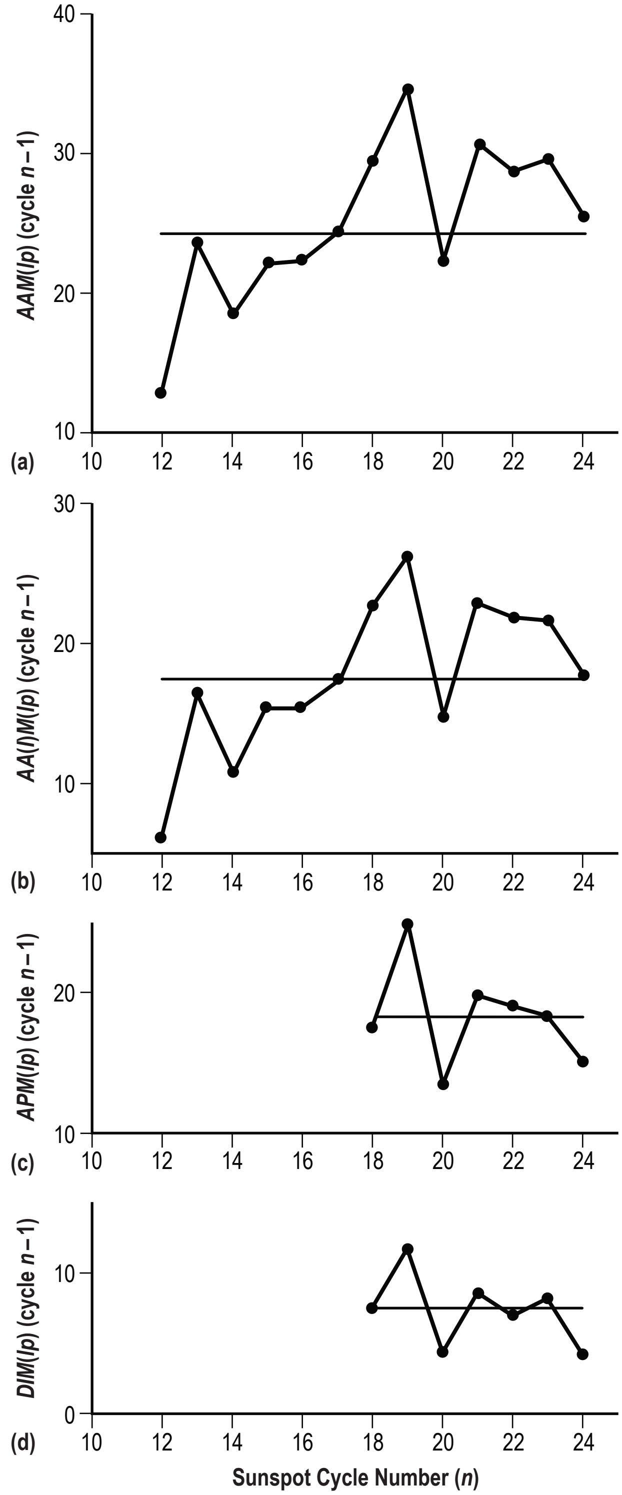

Figure 3. Cyclic variation of selected 12-mma geomagnetic late-peak values for cycles 12–24.

2.3 Single-Variate Fits for Predicting *RM*

Based on figures 2 and 3, it seems highly likely that preferential associations exist between the size of a following cycle's *RM* and, perhaps, *Rm* and at least some of the precursor geomagnetic parameters. Figure 4 depicts the scatter plot of *RM* versus *Rm* for cycles 12–23, often called the maximum-minimum effect.[26] The scatter plot suggests that cycles having larger (smaller) than average *Rm* tend to have larger (smaller) than average *RM*. Ignoring cycle 19, which clearly is a statistical outlier with respect to the maximum-minimum effect, *RM* is found to preferentially associate with *Rm* at the 99.5% confidence level (*cl*), having a coefficient of correlation (*r*) equal to 0.78 and inferring that more than 60% of the variance in *RM* can be explained by the variation in *Rm* alone. The arrow along the *x* axis marks the lowest value of *R* that has been seen thus far (3.3) in late cycle 23. Presuming that this late-cycle value represents *Rm* for cycle 24, cycle 24's *RM* is computed to be about 90 ± 42 (the 90% prediction interval). Ignoring cycle 19, the six cycles having *Rm* ≤5.6 have had maximum amplitudes averaging about 88 ± 21 (±1-*sd* interval) with six of six having *RM* ≤119.2; the average deviation (*ad*) about the mean is about ±19. Thus, unless cycle 24 is a statistical outlier, like cycle 19, its *RM* should be ≤132 and possibly ≤119.

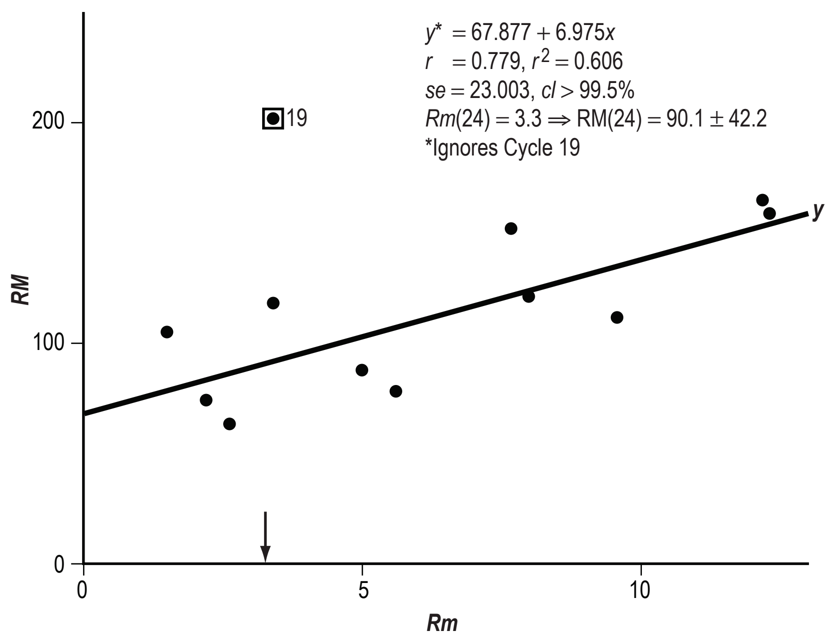

Figure 4. Maximum-minimum effect.

Table 4 gives the results of linear regression analyses comparing *RM* against the geomagnetic precursors identified in table 1, arranged in decreasing order according to the inferred *r*. Of the 13 correlations, all are statistically important, except the last two (*DIM* and *APM*), obviously due to the brevity of the *AP* and *DI* records. Shown in the table are the coefficients of correlation (*r*) and determination (r^2), the *y* axis intercept (*a*), the slope (*b*), the standard error of estimate (*se*), the confidence level (*cl*, where *cl* ≥95% means the inferred regression is considered statistically important), the number of cycles (*n*) used in the analysis, and the predicted maximum amplitude for cycle 24 (*RM*(24), where the ± values give the 90% prediction interval). The inferred correlation having the highest *r* is the one between *RM* and <*ap*(–36)>, having $r = 0.967$ and inferring that 93.5% of the variance in *RM* can be explained by the variation in the average of the 36 monthly *ap* values preceding *Rm* alone; i.e., <*ap*(–36)>. For cycle 24, this relationship predicts cycle 24's *RM* to be quite small, only about 69 ± 20, or having only a 5% chance of being either smaller than 49 or larger than ≈89.

Table 4. Results of linear regression analyses between *RM* and geomagnetic parametric values.

Correlation	*r*	*r*×*r*	a	b	*se*	*cl*	*n*	*RM*(24)#
RM vs. <*ap*(–36)>	0.967	0.935	–56.613	13.382	9.261	>99.8	6	69.2 ± 19.7
RM vs. *AA*(*I*)*m**	0.935	0.874	33.261	10.982	15.617	>99.9	12	123.3 ± 28.3
RM vs. *AAm**	0.926	0.857	–30.492	10.134	16.596	>99.9	12	120.5 ± 30.1
RM vs. <*aa*(*I*)(–36)>	0.911	0.830	24.286	7.053	18.157	>99.9	12	98.3 ± 32.9
RM vs. <*aa*(–36)>	0.906	0.821	–16.407	6.567	18.588	>99.9	12	98.5 ± 33.7
RM vs. <*di*(–36)>	0.905	0.819	47.678	18.718	15.517	>98	6	77.6 ± 33.1
RM vs. *APm*	0.902	0.814	–29.441	18.995	15.186	>99	7	111.1 ± 30.6
RM vs. *AA*(*I*)*M*	0.863	0.746	–58.332	8.697	22.197	>99.9	12	193.0 ± 40.2
RM vs. *DIm*	0.843	0.710	75.293	53.154	18.943	>98	7	101.9 ± 38.2
RM(sum) vs. *di*(sum)	0.827	0.684	98.169	0.351	17.192	>98	6	136.5 ± 36.7
RM vs. *AAM*	0.655	0.429	–50.924	5.759	33.266	>95	12	167.9 ± 60.3
RM vs. *DIM*$	0.442	0.195	62.367	9.557	32.710	<90	6	156.0 ± 69.7
RM vs. *APM*$	–0.061	0.004	166.787	–0.693	36.406	<90	6	161.7 ± 77.6
Weighted mean prediction (weighted by *r*)@: 116.0 ± 34.0								

Notes: Correlations between maximum values compare *RM* values for cycle *n* against maximum values of geomagnetic parameters post *E*(*RM*) for cycle *n* – 1.
* means the geomagnetic parameters are the minimum values in the vicinity of *E*(*Rm*).
\# means the number after ± is the 90% prediction interval for cycle 24's *RM*.
$ means correlations between *RM* and *APM* and *DIM* were not statistically important (*cl* < 95).
RM(sum) means the sum of *RM* values for cycles *n* and *n* + 1.
di(sum) means the sum of di values from *E*(*Rm*) for cycle *n* to *E*(*Rm*) for cycle *n* + 1.
@ means the weighted mean prediction is based only on correlations having *r* > 0.5

The second strongest inferred correlation, having $r = 0.935$ and based on twice as many cycles, is the correlation between *RM* and *AA*(*I*)*m*. Using *AA*(*I*)*m* = 8.2, the lowest value that has been seen thus far (in July 2007; however, it could eventually fall below this value sometime in 2008–2009, based on the usual past behavior of *E*(*AA*(*I*)*m*) relative to *E*(*Rm*)), *RM* for cycle 24 is predicted to be about 123 ± 28. From this inferred preferential relationship, *RM* for cycle 24 is not expected to exceed ≈151, nor is it expected to fall below ≈95. Compared to the preceding prediction based on <*ap*(–36)>, one finds no overlap in the two 90% prediction intervals. This presents a dilemma. Will cycle 24 have *RM* smaller than 89, possibly as low as 49, or larger than 95, possibly as high as 151? Perhaps, the best approach might be to simply average all the statistically important predictions for cycle 24's *RM*, weighting each prediction by its *r*. Doing so, one finds that cycle 24's *RM* should be about 116 ± 34, or having a value somewhere between 82 and 150.

From the table, one finds the highest prediction of cycle 24's *RM* is the one based on *AA*(*I*)*M*, having *r* = 0.863. This inferred preferential regression is statistically important at *cl* ≥99.9% and suggests cycle 24's *RM* will be quite large, about 193 ± 40, inferring only a 5% chance that it will fall below 153 and only a 1% chance of falling below ≈133. It is apparent then that cycle 24 seems destined to be a statistical outlier with respect to one or more of the inferred preferential formulations found in this study.

Figures 5 and 6 display the scatter plots for the inferred statistically important preferential associations between *RM* and the various geomagnetic precursors. The diagonal line in each panel represents the inferred regression line. Also given are *r* and *ad* for each scatter plot, as well as an arrow that marks the parametric value used for predicting cycle 24's *RM*. The strongest regression appears in figure 5(i), *RM* versus <*ap*(–36)>, having *r* = 0.97 and *ad* = 6.1, while the weakest regression appears in figure 5(c), *RM* versus *AAM*, having *r* = 0.65 and *ad* = 27.4.

Table 5 gives the results of linear regression analyses comparing *RM* against the smaller secondary late-peak (*lp*) maxima of the geomagnetic precursors, arranged in decreasing order according to the inferred *r*. Although all the inferred regressions are statistically important, they are not as strong as those based on <*ap*(–36)>, *AA*(*I*)*m*, or *AAm*. The weighted mean prediction based on these *lp* maxima suggests that cycle 24's *RM* will be about 118 ± 36, essentially the same as found for the weighted mean prediction given in table 4.

Figure 7 displays the scatter plots of *RM* versus the geomagnetic precursor late-peak maxima. For each, the diagonal line represents the inferred regression line. Also given are *r* and *ad* for each scatter plot, as well as an arrow that marks the parametric value used for predicting cycle 24's *RM*.

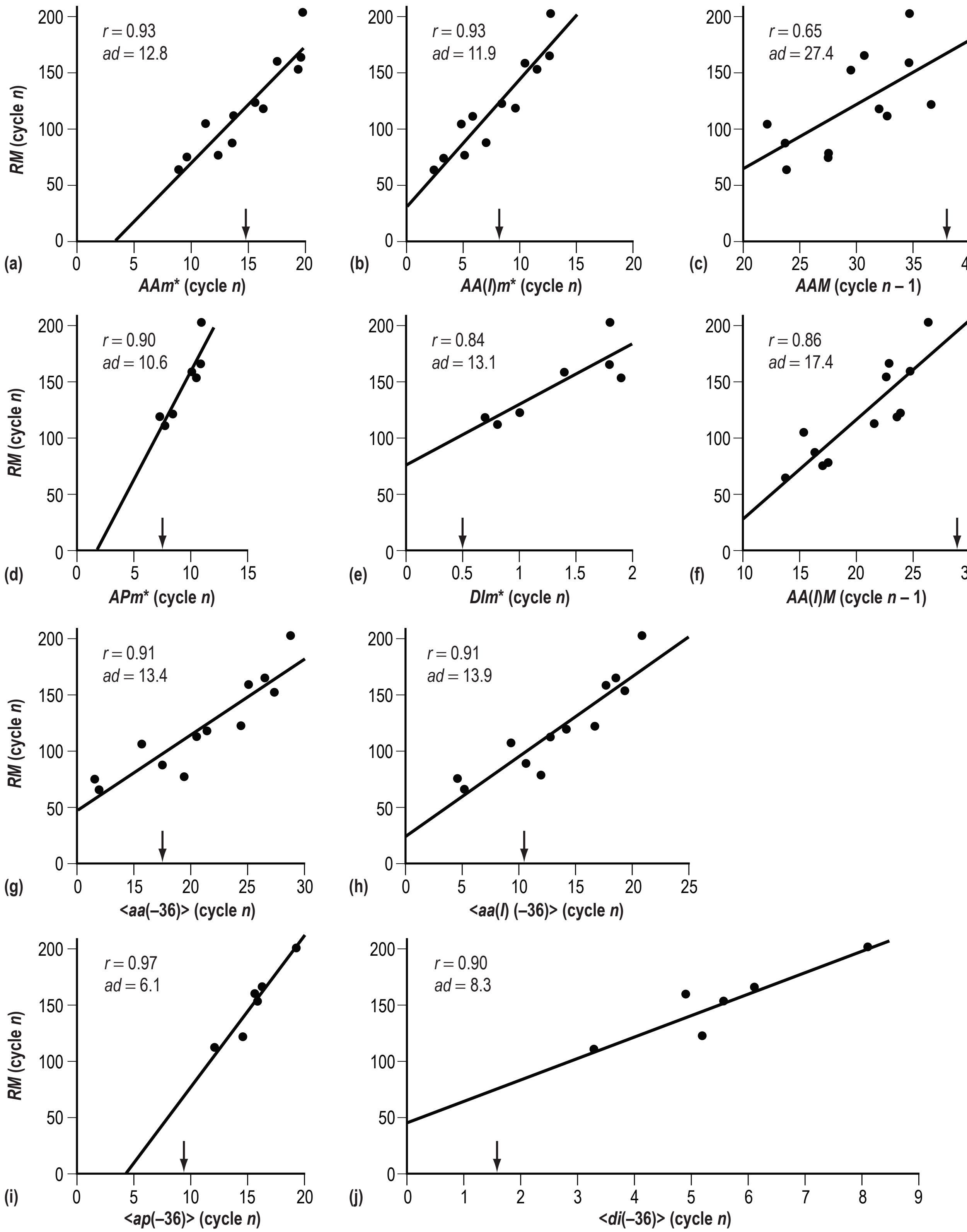

Figure 5. Scatter plots of statistically important single-variate fits.

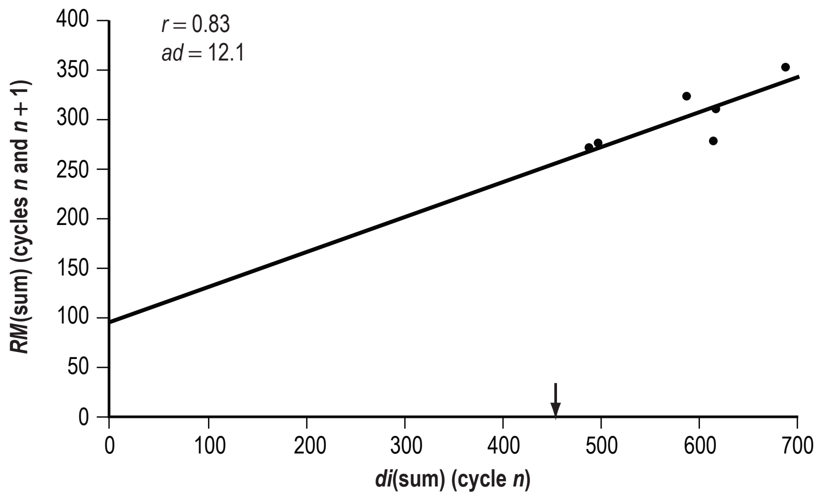

Figure 6. Thompson's method.

Table 5. Results of linear regression analyses between *RM* and late-peak geomagnetic maxima.

Correlation	r	$r \times r$	a	b	se	cl	n	$RM(24)^{\#}$
RM vs. *APM*(*lp*)	0.915	0.837	0.002	8.017	14.645	>98	6	121.1 ± 31.2
RM vs. *AAM*(*lp*)	0.893	0.797	–35.649	6.222	19.795	>99.9	12	121.8 ± 35.9
RM vs. *AAM*(*I*)(*lp*)	0.892	0.795	5.131	6.494	19.884	>99.9	12	119.4 ± 36.0
RM vs. *DIM*(*lp*)	0.845	0.714	62.404	11.391	19.466	>95	6	109.1 ± 41.5
Weighted mean prediction (weighted by *r*): 118.0 ± 36.0								

Notes: # means the number after ± is the 90% prediction interval for cycle 24's *RM*
lp means "late peak"

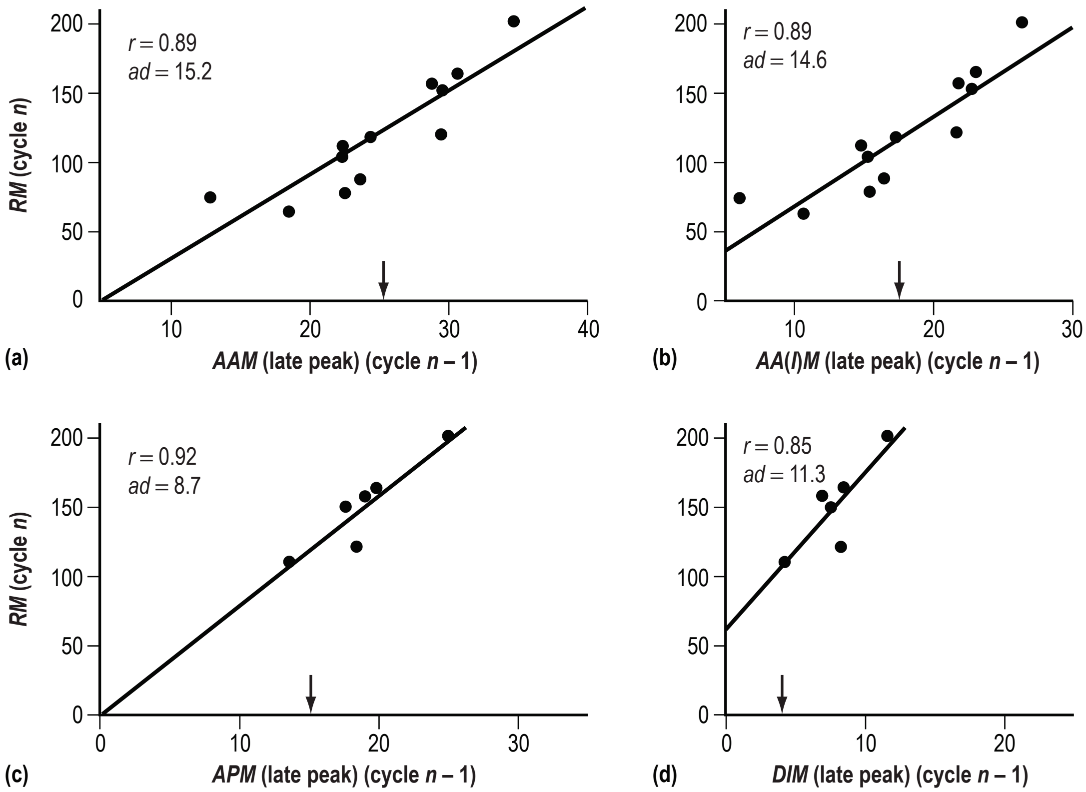

Figure 7. Scatter plots of statistically important late-peak, single-variate fits.

2.4 Bi-Variate Fits for Predicting *RM*

Table 6 gives the results of bi-variate regression analyses[27] (of the form, $y = a + b_1x_1 + b_2x_2$), comparing *RM* against various combinations of minimum and maximum precursor values, arranged in decreasing order of the inferred *r*. Whereas, the best single-variate regression has $r = 0.967$ and $se = 9.3$, the best bi-variate regression has slightly higher *r* and lower *se*, being 0.981 and 8.2, respectively. It predicts cycle 24's *RM* to be about 92 ± 27. The weighted mean prediction of the 22 correlations having $r > 0.5$ is about 112 ± 32, slightly lower than found for the single-variate predictions.

Figure 8 compares the bi-variate predictions of *RM* against the observed values of *RM*, using those bi-variate fits having $r \geq 0.925$. The diagonal lines are the 1:1 lines and the arrows denote the predicted values for cycle 24's *RM*. The bi-variate fit having the smallest *ad* appears in figure 8(c), *RM* versus <*ap*(–36)>, having $r = 0.97$ and $ad = 5.2$. It predicts cycle 24's *RM* to be about 57 ± 23 (the 90% prediction interval).

Table 6. Results of bi-variate regression analyses ($y = a + b_1 x_1 + b_2 x_2$).

Correlation	r	$r \times r$	a	b_1	b_2	se	n	RM(24)[$]
RM vs. APM[#], APm*	0.981	0.962	–203.346	4.514	26.344	8.157	6	92.3 ± 27.3
RM vs. APM(lp), APm*	0.976	0.952	–56.404	4.622	12.525	9.211	6	106.1 ± 21.7
RM vs. Rm, <ap(–36)>	0.973	0.947	–81.539	1.259	14.268	9.673	6	56.7 ± 22.8
RM vs. DIM[#], DIm*	0.967	0.936	–39.598	11.056	60.707	10.660	6	99.1 ± 25.1
RM vs. Rm, APm*	0.966	0.932	–23.363	–3.127	21.067	10.232	7	122.2 ± 21.8
RM vs. AA(I)M(lp), AA(I)m*	0.939	0.882	23.573	1.610	8.604	15.952	12	122.5 ± 29.2
RM vs. AA(I)M[#], AA(I)m*	0.938	0.881	11.084	1.792	9.140	16.011	12	137.8 ± 29.3
RM vs. Rm, AA(I)m*	0.938	0.879	34.667	–0.971	11.559	16.124	12	126.2 ± 29.6
RM vs. AAM(lp), AAm*	0.932	0.869	–37.288	1.890	7.407	16.785	12	120.9 ± 23.2
RM vs. Rm, AAm*	0.931	0.867	–33.838	–1.353	10.918	16.891	12	124.4 ± 31.0
RM vs. Rm, <di(–36)>	0.926	0.858	9.128	2.427	21.796	15.865	6	52.0 ± 37.3
RM vs. AAM[#], AAm*	0.925	0.856	–39.975	0.553	9.668	17.567	12	125.1 ± 32.2
RM vs. Rm, APM(lp)	0.921	0.848	–20.424	1.163	8.553	16.418	6	112.6 ± 35.0
RM vs. Rm, <aa(I)(–36)>	0.919	0.844	24.862	–1.625	7.746	18.332	12	100.8 ± 33.6
RM vs. DIM(lp), DIm*	0.918	0.843	46.569	7.241	33.242	16.682	6	92.9 ± 39.3
RM vs. Rm, <aa(–36)>	0.913	0.835	–20.034	–1.645	7.228	18.848	12	101.0 ± 34.5
RM vs. Rm, AAM(lp)	0.893	0.797	–35.426	0.118	6.184	20.877	12	121.4 ± 28.9
RM vs. Rm, AA(I)M(lp)	0.892	0.795	5.134	–0.047	6.509	20.996	12	119.5 ± 29.0
RM vs. Rm, DIm*	0.875	0.766	88.598	–2.087	55.815	19.053	7	109.6 ± 44.8
RM vs. Rm, AA(I)M[#]	0.864	0.746	–59.800	–0.340	8.871	23.358	12	197.7 ± 42.8
RM vs. Rm, DIM(lp)	0.863	0.746	28.041	2.214	13.280	21.229	6	89.8 ± 45.3
RM vs. Rm, AAM[#]	0.647	0.419	–40.221	1.487	5.091	34.667	12	158.1 ± 62.8
RM vs. Rm, DIM[#]	0.467	0.218	101.224	–1.838	7.132	37.222	6	165.1 ± 87.6
RM vs. Rm, APM[#]	0.435	0.190	246.103	–4.488	–2.454	37.885	6	176.6 ± 89.1
Weighted mean prediction (weighted by r)[@]: 112.1 ± 32.4								

Notes: [$] means 90% prediction interval.
[#] means the maximum after E(RM).
* means the minimum in the vicinity of E(Rm).
lp means late peak.
[@] means the weighted mean prediction is based only on correlations having $r > 0.5$.

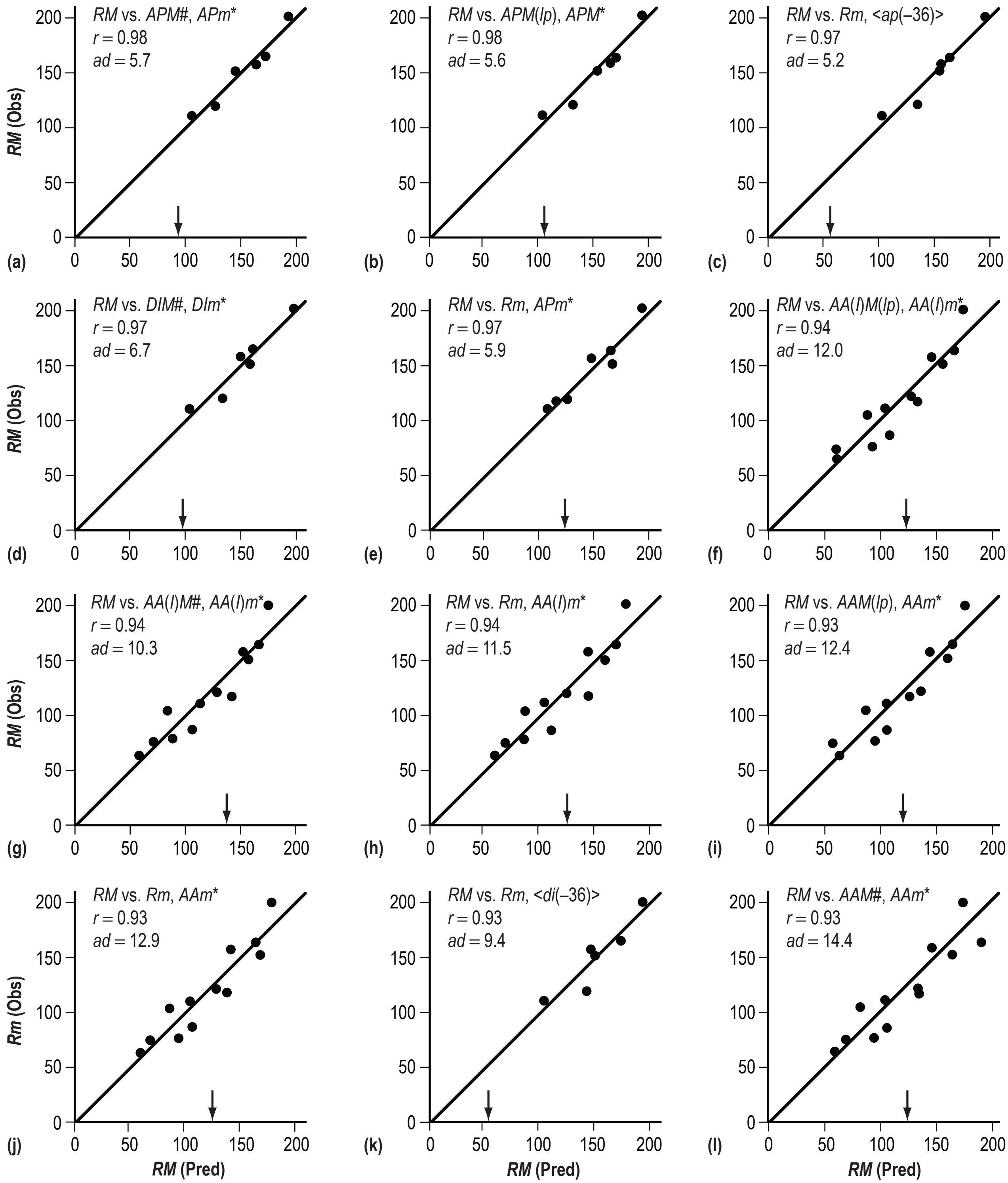

Figure 8. Scatter plots of selected bi-variate fits having $r \geq 0.925$.

2.5 Late-Cycle Parametric Values for Cycle 23 in Comparison to Near Cycle Minimum Means for Cycles 20–23 ($-12 \le t \le 24$) and for Cycle 14 ($-20 \le t \le 20$)

Table 7 gives late-cycle 12-mma parametric values for cycle 23, from January 2006 through April 2008. Shown are the year and month, *t*, *R*, *V*, *AA*, *AA*(*I*), *AP*, and *DI*. Tentative minimum values have been seen during this 28-mo interval in *V* (April 2006) and in *AA*, *AA*(*I*), *AP*, and *DI* (July 2007). Table 8 gives the 12-mma for the same parameters, but for the interval $-12 \le t \le 24$ about *E*(*Rm*), individually for cycles 20–23 and for the mean of cycles 20–23.

Table 7. Late-cycle parametric values for cycle 23, January 2006 through April 2008.

Year	Month	*t*	*R*	*V*	*AA*	*AA*(*I*)	*AP*	*DI*
2006	01	116	20.8	436.5	17.9	10.6	9.7	1.8
2006	02	117	18.6	431.7	17.1	10.0	9.2	1.6
2006	03	118	17.4	425.4	16.2	9.1	8.5	1.3
2006	04	119	17.1	423.4*m*	15.5	8.4	8.0	1.0
2006	05	120	17.3	424.0	15.6	8.5	8.0	1.1
2006	06	121	16.3	425.8	15.9	8.8	8.3	1.4
2006	07	122	15.3	431.2	16.4	9.4	8.7	1.6
2006	08	123	15.6	435.8	16.7	9.7	8.9	1.7
2006	09	124	15.6	438.2	16.7	9.7	8.9	1.6
2006	10	125	14.2	439.8	16.7	9.8	8.8	1.4
2006	11	126	12.6	441.4	16.7	9.9	8.8	1.4
2006	12	127	12.1	441.5	16.7	9.8	8.8	1.5
2007	01	128	11.9	441.6	16.6	9.8	8.7	1.4
2007	02	129	11.5	443.5	16.5	9.7	8.5	1.3
2007	03	130	10.7	446.1	16.4	9.6	8.5	1.2
2007	04	131	9.9	447.6	16.3	9.6	8.5	1.2
2007	05	132	8.7	447.7	16.1	9.4	8.3	1.1
2007	06	133	7.7	444.9	15.5	8.8	7.9	0.8
2007	07	134	7.0	442.3	14.9*m*	8.2*m*	7.4*m*	0.5
2007	08	135	6.0	446.8	15.1	8.5	7.5	0.5
2007	09	136	5.9	454.0	15.7	9.1	7.8	0.6
2007	10	137	6.0	460.3	15.9	9.3	7.9	0.7
2007	11	138	5.7	463.6	15.8	9.2	7.8	0.6
2007	12	139	4.9	466.3	15.8	9.3	7.8	0.5
2008	01	140	4.2	468.6	15.8	9.3	7.8	0.5
2008	02	141	3.5	467.0	–	–	7.6	0.5
2008	03	142	3.3	–	–	–	–	–
2008	04	143	3.3	–	–	–	–	–

Notes: *t* = elapsed time in months from cycle 23's *E*(*Rm*), which occurred in 05 1996 and measured 8.0.
R = 12 mma of monthly mean sunspot number.
V = 12 mma of the monthly mean solar wind speed (in km/s).
AA = 12 mma of the monthly mean *aa*-geomagnetic index (in nT).
AA(*I*) = 12 mma of the monthly mean interplanetary component of the aa index (in nT).
AP = 12 mma of the *ap*-geomagnetic index (in nT).
DI = 12 mma of the monthly mean disturbance index (the number of days when *ap* equals or exceeds 25 nT).
m = minimum parametric value.

Table 8. Selected parametric values and averages for cycles 20–23 near $E(Rm)$.

	R					***V***					***AA***				
t	**20**	**21**	**22**	**23**	**Mean**	**20**	**21**	**22**	**23**	**Mean**	**20**	**21**	**22**	**23**	**Mean**
–12	26.0	16.0	17.3	19.2	19.6	–	483.0	489.2	436.8	469.7	22.3	24.0	23.6	22.7	23.2
–11	23.8	15.0	17.3	18.2	18.6	–	481.0	486.7	433.9	467.2	22.3	23.5	23.1	22.2	22.8
–10	21.3	14.3	16.8	17.0	17.4	–	477.0	484.7	429.8	463.8	22.0	23.3	22.6	21.8	22.4
–9	19.5	14.4	15.3	15.4	16.2	–	474.5	484.4	428.8	462.6	21.6	23.2	22.5	21.4	22.2
–8	17.8	15.4	13.8	13.4	15.1	–	473.0	479.0	427.7	459.9	21.1	23.3	22.1	21.2	21.9
–7	15.4	16.1	13.1	12.1	14.2	–	470.9	474.7	426.6	457.4	19.9	23.4	21.8	21.0	21.5
–6	12.7	16.3	13.0	11.3	13.3	–	468.6	475.6	422.5	455.6	18.7	23.3	21.9	20.1	21.0
–5	10.8	15.2	13.7	10.8	12.6	–	466.0	477.1	415.4	452.8	18.1	23.0	21.9	19.1	20.5
–4	10.2	13.2	14.3	10.4	12.0	–	463.4	474.0	412.5	450.0	17.5	22.9	21.7	18.7	20.2
–3	10.3	12.2	13.8	10.1	11.6	–	463.5	467.8	413.3	448.2	16.8	23.1	21.3	18.8	20.0
–2	10.2	12.6	13.7	9.7	11.6	–	465.0	459.6	416.6	447.1	16.3	23.4	20.7	19.0	19.9
–1	9.9	12.5	13.2	8.5	11.0	–	462.1	448.5	420.7	443.8	15.8	22.9	19.4	19.0	19.3
0	9.6	12.2	12.3	8.0	10.5	–	454.8	442.9	422.7	440.1	15.2	22.3	18.3	18.8	18.7
1	10.2	12.9	13.2	8.5	11.2	–	448.5	440.0	423.9	437.5	14.5	22.0	18.1	18.7	18.3
2	11.0	16.4	14.9	8.4	12.7	–	443.3	434.3	424.0	433.9	14.2	21.5	17.8	18.5	18.0
3	11.7	14.3	16.3	8.3	12.7	434.9	435.4	430.8	422.0	430.8	14.2	20.6	17.5	18.5	17.2*m*
4	12.0	13.5	17.6	8.4	12.9	431.1	429.1	428.6	418.7	426.9	14.2	20.0	17.5*m*	18.2	17.5
5	12.5	13.5	19.6	8.8	13.6	429.4	425.9	425.8	415.3	424.1	14.2	19.9	17.7	17.9	17.4
6	13.6	14.8	22.1	9.8	15.1	426.4	422.7	424.1	412.3	421.4	14.0	19.6	18.0	17.8	17.4
7	14.6	16.7	24.4	10.4	16.5	422.2	420.8	424.1	411.1	419.6	13.8	19.6*m*	18.5	18.0	17.5
8	15.2	18.1	26.5	10.5	17.6	420.2	423.0	427.6	410.3	420.3	13.8*m*	20.1	18.9	18.1	17.7
9	15.5	20.0	28.4	11.0	18.7	421.6	424.5	431.6	407.4	421.3	14.1	20.3	18.9	17.9	17.8
10	16.4	22.2	31.3	13.5	20.9	422.1	423.0	432.0	401.6	419.7	14.1	20.2	19.2	17.6	17.8
11	17.4	24.2	34.8	16.5	23.2	420.3	421.7	428.7	394.4	416.3	14.2	20.3	19.8	17.1	17.9
12	19.7	26.3	39.0	18.3	25.8	418.9	419.4	423.8*m*	389.8	413.9	14.4	20.2	20.3	16.5	17.9
13	22.3	29.0	43.6	20.3	28.8	417.0	418.0	425.7	385.4	411.5	14.6	20.4	21.0	16.4	18.1
14	24.5	33.4	46.7	22.6	31.8	414.3	417.0*m*	434.0	380.5	411.5*m*	14.6	20.9	21.8	16.3	18.4
15	27.7	39.1	51.3	25.0	35.8	413.1	418.0	439.2	377.3	411.9	14.6	21.3	22.2	16.0	18.5
16	31.3	45.6	58.2	28.3	40.9	412.4*m*	421.9	441.6	376.5	413.1	14.8	21.9	22.5	15.8	18.8
17	34.5	51.9	64.6	31.8	45.7	414.2	426.0	442.2	376.4*m*	414.7	15.4	22.6	22.4	15.8*m*	19.1
18	37.4	56.9	71.3	35.0	50.2	417.5	429.8	439.0	380.0	416.6	16.1	23.6	21.9	16.0	19.4
19	40.7	61.3	77.5	39.0	54.6	420.7	429.1	435.4	385.7	417.7	16.5	24.1	21.5	16.5	19.7
20	44.7	64.5	83.8	43.7	59.2	425.3	423.7	430.5	389.2	417.2	17.0	24.1	21.4	17.9	20.1
21	50.3	69.6	93.7	48.9	65.6	425.9	421.5	429.0	393.0	417.4	17.5	24.4	21.8	18.7	20.6
22	56.7	76.9	104.3	53.4	72.8	423.6	423.0	437.0	395.3	419.7	17.9	24.5	22.6	19.4	21.1
23	63.1	83.2	113.7	56.5	79.1	420.5	426.0	447.2	399.3	423.3	17.9	24.8	23.2	19.7	21.4
24	67.6	89.3	121.2	59.4	84.4	418.1	431.3	457.0	404.2	427.7	17.8	25.3	24.8	20.2	22.0

Table 8. Selected parametric values and averages for cycles 20–23 near $E(Rm)$ (Continued).

	***AA*(*I*)**					***AP***					***DI***				
t	**20**	**21**	**22**	**23**	**Mean**	**20**	**21**	**22**	**23**	**Mean**	**20**	**21**	**22**	**23**	**Mean**
–12	14.8	17.0	16.6	15.5	16.0	13.5	14.1	14.7	13.8	14.0	3.9	5.1	4.1	4.9	4.5
–11	14.9	16.6	16.0	15.1	15.7	13.5	13.8	14.2	13.4	13.7	4.1	5.0	3.9	4.8	4.5
–10	14.7	16.3	15.5	14.7	15.3	13.4	13.7	13.8	13.0	13.5	4.2	4.6	3.7	4.6	4.3
–9	14.4	16.2	15.5	14.4	15.1	13.2	13.8	13.8	12.6	13.4	4.0	4.6	3.7	4.1	4.1
–8	14.0	15.3	15.1	14.3	14.7	12.9	14.0	13.4	12.2	13.1	3.8	4.5	3.5	3.5	3.8
–7	12.9	16.3	14.9	14.1	14.6	12.0	14.0	13.1	11.8	12.7	3.4	4.4	3.3	3.3	3.6
–6	11.8	16.2	15.0	13.3	14.1	11.0	14.0	13.3	11.5	12.5	2.9	4.3	3.3	2.8	3.3
–5	11.3	16.0	15.0	12.3	13.7	10.6	13.9	13.3	10.8	12.2	2.6	4.1	3.3	2.3	3.1
–4	10.7	16.0	14.7	12.0	13.4	10.2	13.7	13.1	10.0	11.8	2.3	4.0	3.2	2.1	2.9
–3	10.0	16.3	14.4	12.0	13.2	9.7	13.8	12.8	9.7	11.5	2.0	4.0	3.0	2.0	2.8
–2	9.5	16.5	13.8	12.3	13.0	9.3	13.9	12.3	9.7	11.3	1.9	4.0	2.6	2.2	2.7
–1	9.1	16.0	12.5	12.3	12.5	9.0	13.5	11.4	9.8	10.9	1.7	3.8	2.0	2.1	2.4
0	8.4	15.4	11.4	12.1	11.8	8.5	13.1	10.5	9.7	10.5	1.5	3.4	1.7	1.9	2.1
1	7.7	15.1	11.2	12.0	11.5	8.2	12.9	10.4	9.5	10.3	1.3	3.3	1.6	1.8	2.0
2	7.4	14.5	10.9	11.8	11.2	8.0	12.5	10.2	9.4	10.0	1.2	3.0	1.5	1.8	1.9
3	7.3	13.7	10.5	11.8	10.8	8.0	11.8	10.0	9.3	9.8	1.2	2.4	1.4*m*	1.8	1.7
4	7.3	13.1	10.4*m*	11.5	10.6	8.0	11.2	10.0*m*	9.3	9.6	1.1	2.0	1.5	1.8	1.6
5	7.4	13.0	10.5	11.2	10.5	8.0	11.0	10.2	9.2	9.6	1.0	1.9	1.5	1.6	1.5
6	7.1	12.6	10.7	11.1	10.4	7.9	10.8*m*	10.3	9.0	9.5*m*	0.9	1.8	1.7	1.5	1.5*m*
7	6.8*m*	12.6*m*	11.1	11.2	10.4	7.7*m*	11.0	10.6	9.0	9.6	0.8	1.8*m*	2.1	1.6	1.6
8	6.9	12.9	11.3	11.2	10.6	7.8	11.3	10.8	9.2	9.8	0.8*m*	2.1	2.3	1.7	1.7
9	7.1	13.1	11.3	10.9	10.6	7.9	11.6	10.9	9.2	9.9	0.9	2.3	2.4	1.6	1.8
10	7.1	12.9	11.5	10.2	10.4	7.9	11.8	11.1	9.1	10.0	0.9	2.4	2.7	1.3	1.8
11	7.2	12.9	11.9	9.5	10.4	8.0	11.9	11.5	8.8	10.1	1.0	2.5	3.0	1.0*m*	1.9
12	7.2	12.8	12.2	9.3	10.4*m*	8.2	11.9	11.9	8.5	10.1	1.0	2.6	3.3	1.1	2.0
13	7.2	12.8	12.7	9.1	10.5	8.3	12.1	12.5	8.5	10.4	1.0	2.8	3.7	1.2	2.2
14	7.2	12.9	13.3	8.8	10.6	8.3	12.5	13.0	8.5	10.6	0.9	3.0	3.8	1.2	2.2
15	7.0	12.8	13.6	8.4	10.5	8.1	13.0	13.3	8.4	10.7	0.9	3.3	3.9	1.1	2.3
16	7.0	13.1	13.5	8.3	10.5	8.3	13.5	13.5	8.2*m*	10.9	1.0	3.7	3.9	1.2	2.5
17	7.5	13.5	13.1	8.3*m*	10.6	8.8	14.3	13.3	8.3	11.2	1.0	4.1	3.8	1.4	2.6
18	8.1	14.3	12.3	8.7	10.9	9.4	15.4	12.9	8.5	11.6	1.3	4.8	3.4	1.6	2.8
19	8.3	14.6	11.6	9.3	11.0	9.8	15.9	12.5	8.9	11.8	1.5	5.0	2.9	1.8	2.8
20	8.6	14.4	11.2	9.6	11.0	10.1	16.0	12.3	9.5	12.0	1.7	5.1	2.8	1.9	2.9
21	8.8	14.5	11.1	10.2	11.2	10.5	16.3	12.4	9.8	12.3	1.9	5.2	2.8	2.3	3.1
22	9.0	14.3	11.5	10.6	11.4	10.8	16.3	12.8	10.5	12.6	2.1	5.2	3.1	2.5	3.2
23	8.7	14.3	11.9	10.7	11.4	10.7	16.5	13.1	11.0	12.8	2.1	5.1	3.3	2.6	3.3
24	8.4	14.5	13.3	11.1	11.8	10.5	16.8	14.3	11.3	13.2	2.0	5.3	3.7	2.7	3.4

Figure 9 compares late cycle 23 12-mma parametric values (the filled circles, which presume sunspot minimum for cycle 24 in March 2008, as per the National Oceanic and Atmospheric Administration (NOAA) Solar Cycle Prediction Panel's prediction[28] for onset of cycle 24, actually March 2008 ± 6 mo) with parametric mean values for cycles 20–23. The arrows mark the minimum values of the parametric means, and the individual epochs of cycle parametric minimum values are identified. The asterisks (*) simply denote that the parametric values used are the minimum values in the vicinity of cycle minimum.

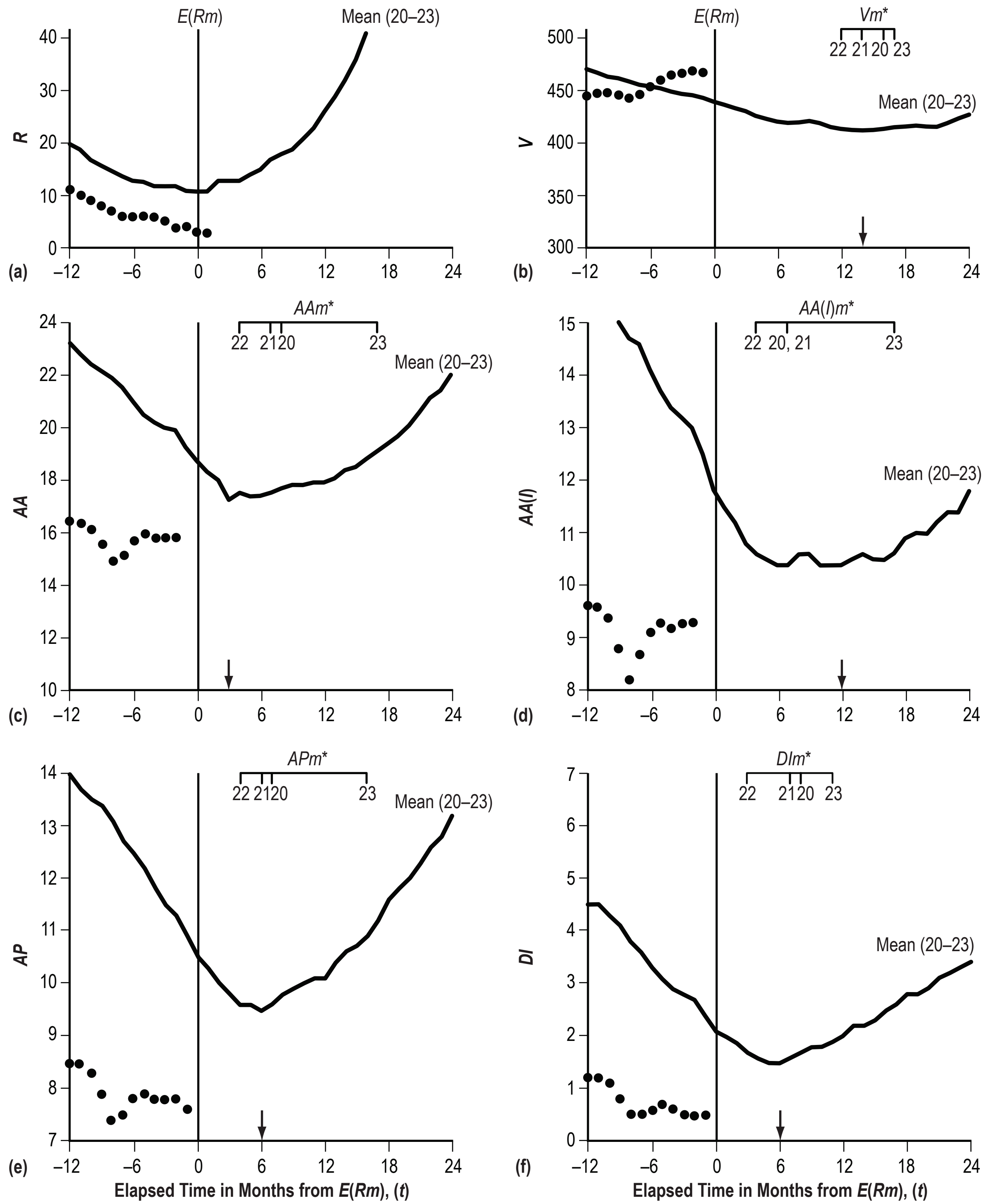

Figure 9. Comparison late-cycle 23 values with cycles 20–23 mean values for $-12 \le t \le 24$ mo, where t is the elapsed time in months from $E(Rm)$.

For *R*, *AA*, *AA*(*I*), *AP,* and *DI*, all values for late cycle 23 appear well below the means of cycles 20–23. For *AA*, the mean is at minimum value at $t = 3$ mo past *E*(*Rm*), although individual cycle minimums are found to occur between $t = 4$ and 17 mo past *E*(*Rm*). For *AA*(*I*), the mean is at minimum value at $t = 12$ mo past *E*(*Rm*), although individual cycle minimums are found to occur between $t = 4$ and 17 mo past *E*(*Rm*). For *AP*, the mean is at minimum value at $t = 6$ mo past *E*(*Rm*), although individual cycle minimums are found to occur between $t = 4$ and 16 mo past *E*(*Rm*). And for *DI*, the mean is at minimum value at $t = 6$ mo past *E*(*Rm*), although individual cycle minimums are found to occur between $t = 3$ and 11 mo past *E*(*Rm*).

For *V*, late cycle 23 values have risen above the mean of cycles 20–23, which is at minimum value at $t = 14$ mo, with individual cycle minimums occurring between 12 and 17 mo past *E*(*Rm*). If the recent burst in solar activity (November 2008) continues and is sustained, then *R*, undoubtedly, will begin to rise, indicating that the epoch of sunspot minimum amplitude for cycle 24 might indeed be March–April 2008. For cycle 24 not to be considered a statistical outlier with respect to cycles 20–23, its geomagnetic parametric values would have to drop below pre-(*E*(*Rm*)) minimum values. If cycle 24 minimum is yet to occur; i.e., occurring post-March 2008, then the filled circles will have to be moved leftward, month by month, to properly adjust for comparison to the mean values for cycles 20–23. Certainly, *DI* cannot get much smaller, since it already is at the lowest value ever seen (0.5). Whether geomagnetic parametric minimums have already been seen or are yet to occur will not be explicitly known for several more months, probably in late 2008 to early 2009.

Figure 10 compares late cycle 23 12-mma parametric values (the filled circles) with those of cycle 14, the weakest cycle in the modern era, having $R = 64.2$. Interestingly, current values of *R* are nearly the same as was seen in cycle 14, and the long-term persistent flattening that was seen in cycle 14 in *AA* and *AA*(*I*), with pre-*E*(*Rm*) minimums, seems similar to late cycle 23 values, although *AA* and *AA*(*I*) values are off-set high for late cycle 23. Because of the strong preferential associations between *RM* and the minimums in *AA* and *AA*(*I*), one speculates that cycle 24's *RM* might lie somewhere between that of cycle 14 (64.2) and cycle 20 (110.6), since cycle 24 minimum values will lie above that of cycle 14 and below that of cycle 20; i.e., about 87 ± 23, or essentially the same as is suggested by the best of all bi-variate fits, $RM = -203.346 + 4.514APM + 26.344APm$, having $r = 0.981$, $se = 8.157$, and $RM(24) = 92.3 \pm 27.3$.

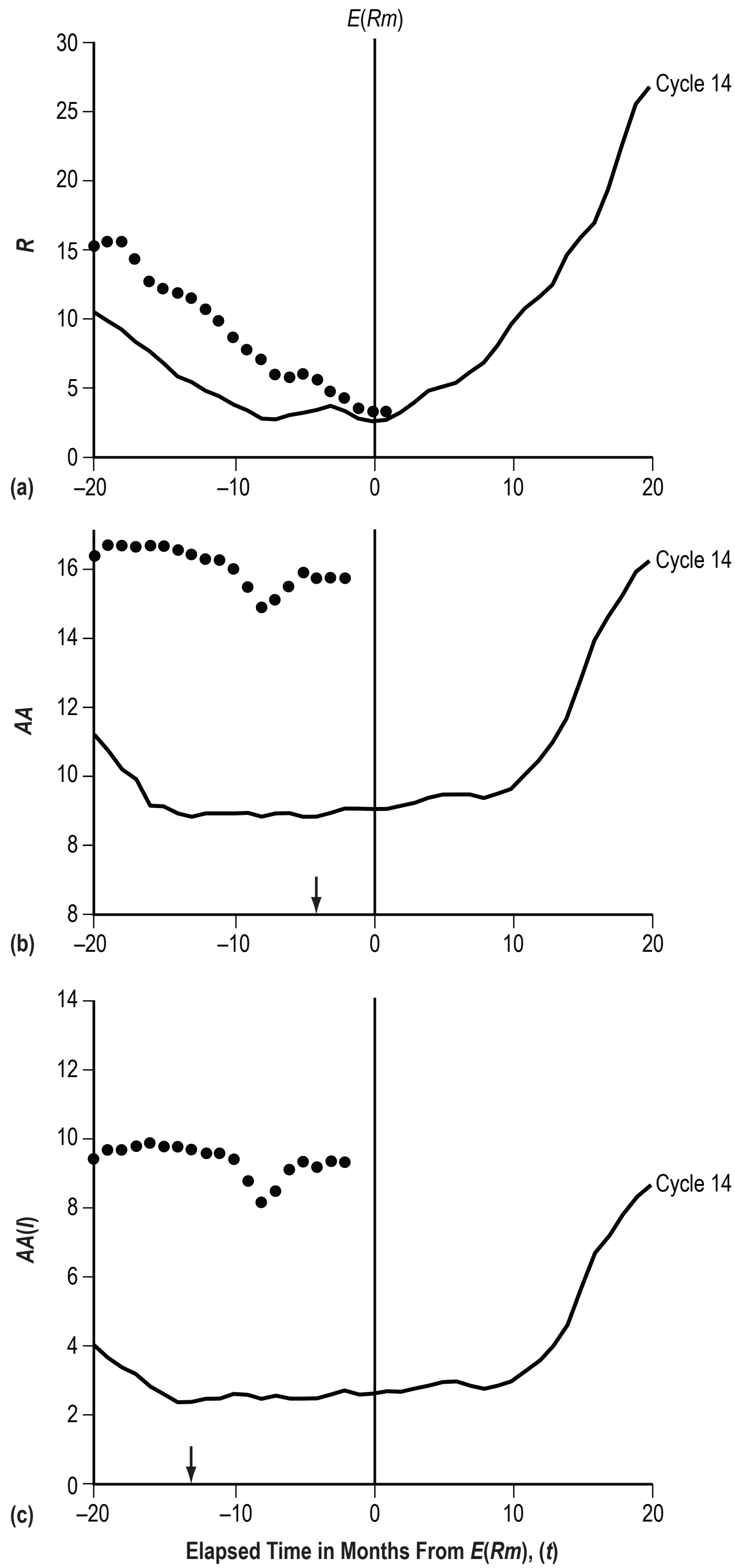

Figure 10. Comparison of late-cycle 23 values with cycle 14 values for $-20 \leq t \leq 20$.

3. DISCUSSION AND SUMMARY

Predicting the size of a sunspot cycle years in advance remains somewhat problematic, being more of an art; i.e., just plain luck, than a science. Attempts to predict the size of a sunspot cycle on the basis of inferred spectral properties in the sunspot record are notoriously bad. For example, Berger et al.[29] forecast cycle 22 (158.5) to have a maximum amplitude of ≈95 on the basis of a generalized harmonic analysis, too low by ≈67%. Also, using spectral peaks deduced from a simple maximum entropy method and multiple regression analysis, Kane[4] predicted the size of cycle 23 to be about 140 ± 9, somewhat higher than its observed value (120.8). As noted earlier, the maximum-minimum effect usually works, although there always seems to be at least one cycle that proves to be a statistical outlier (cycle 19). For even-odd cycle pairs, there is the Gnevyshev-Ohl Rule,[30,31] which predicts that the odd-following cycle in even-odd cycle pairs usually is the bigger cycle, true for 10 of 14 even-odd cycle pairs based on cycles –4 to 23 (however, failing for the most recent cycle pair 22–23). Unfortunately, no such statistically important odd-even cycle pairing has been seen, although one may eventually be revealed, especially if the trend in solar activity is now downward following a possible peak in solar activity about cycles 18–21 (the even-following cycle has been the smaller for two consecutive odd-even cycle pairs 19–20 and 21–22). Presuming that a real downward trend is now underway and that the even-following cycle is usually the smaller in odd-even cycle pairs, then one speculates that cycle 24, perhaps, could have an *RM* about 24%–45% smaller than was seen in cycle 23 (120.8), or measuring about 66–92.

It has long been hoped that a method of prediction, based on physical features related to solar dynamo physics, might be revealed, which would allow more precise prediction of the size and timing of sunspot cycles, perhaps, years in advance. Unfortunately, no such prediction method has yet been identified that consistently and accurately describes the many vagaries associated with solar activity cycles.

Regarding the prediction of cycle 24's *RM*, using an extrapolation of spectral peaks, Kane[4] has predicted cycle 24 to have a maximum of 105 ± 9, peaking in 2010–2011. On the basis of timing predictors (polar field reversal and the butterfly diagram), Schatten[32] has proposed $RM(24) = 120 \pm 40$, peaking in April 2011, while on the basis of certain statistical characteristics, Wang et al.[33] have predicted $RM(24) = 101 \pm 18$. Presuming that solar activity is now in decline starting about 1993, Duhau[34] has predicted $RM(24) = 88 \pm 24$, and presuming a continuing downward trend in solar activity, Sello[35] has predicted $RM(24) = 115 \pm 21$. On the basis that a deep meridional flow drives the solar activity cycle, Hathaway et al.[36,37] have predicted that cycle 24 should be an above average-size cycle, while on the basis of the strength of the polar fields during the declining phase of the sunspot cycle, Svalgaard et al.[38] have predicted $RM(24) = 75 \pm 8$, making it, potentially, the smallest cycle in 100 yr. Using the *aa*-index, Jain[39] has predicted $RM(24) = 144 \pm 18$, while using a flux-transport, dynamo-based model, Dikpati et al.[40] have predicted cycle 24 to have a peak about 30%–50% higher than was seen in cycle 23, or about 169 ± 12. On the basis of the interplanetary peak of the *aa*-index during the declining portion of cycle 23 (in 2003), Hathaway and Wilson[41] have predicted $RM(24) = 160 \pm 25$, or about the size of cycles 21 and 22, although Wilson and Hathaway[16] have also noted that use of the later-occurring smaller secondary peak of 2005 yields a smaller maximum amplitude for cycle 24. On the basis of a specific solar dynamo model, Choudhuri et al.[42] have predicted cycle 24 to have a maximum amplitude about 35% smaller than was seen in cycle 23, or measuring about 80. Obridko and Shelting[43] have noted that predictions based on the polar field and extrapolation of local fields suggest that cycle 24 will be smaller than was seen in cycle 23, while predictions based on the recurrence index and global fields suggest that cycle 24 will be somewhat larger than was seen in cycle 23. On the basis of solar cycles being modeled as a forced and damped harmonic oscillator, Hiremath[44] has predicted that cycle 24 will begin sometime between May and September 2008, having a peak of about 110 ± 11 and a period of only 9.34 yr (112 mo). Using the disturbance index, Dabas et al.[22] have predicted *RM*(24) = 124 ± 23, peaking about 45 ± 4 mo past *E*(*Rm*), probably about mid to late 2011. Wilson and Hathaway[23] have extended the Dabas et al. method to other geomagnetic indices (*AA*, *AA*(*I*), and *AP*) and have predicted *RM*(24) = 130 ± 14, peaking before April 2012, presuming an onset for cycle 24 in March 2008. Wilson and Hathaway[12] also have noted that if, in the course of its rise, cycle 24's 12-mma of the weighted mean latitude of spot groups (weighted by sunspot area) exceeds 24 deg, then cycle 24's *RM* >131, and if the 12-mma of the highest spot group exceeds 38 deg, then cycle 24's *RM* >127. On the basis of the sums of sunspot areas in specific latitude intervals and time intervals, Javaraiah[45,46] has predicted *RM*(24) = 74 ± 10, 103 ± 10, and 87 ± 7. Finally, on the basis of the amplitude-period relationship; i.e., smaller cycles usually following longer period cycles and larger cycles usually following shorter period cycles, Wilson and Hathaway[13] have predicted *RM*(24) ≤96 ± 55 (using all cycle pairs) or ≤91 ± 37 (ignoring certain statistical outlier cycle pairs).

This TP has examined a number of both single- and bi-variate predictors of the maximum amplitude of a sunspot cycle, based on precursor solar and geomagnetic information. Using the maximum-minimum effect and presuming that cycle 24 is not a statistical outlier, because *R* is at or near *Rm* (≈3.3), one predicts *RM*(24) = 90 ± 42 (the 90% prediction interval). Hence, there is only a 5% chance that cycle 24's *RM* will be either smaller than 48 or larger than 132. Using the best single-variate fit (*RM* = –56.613 + 13.382 <*ap*(–36)>), having $r = 0.967$ and $se = 9.3$, one estimates *RM*(24) = 69 ± 20 (the 90% prediction interval), suggesting only a 5% chance that cycle 24's *RM* will be smaller than 49 or larger than 89. However, using the second best single-variate fit (*RM* = 33.261 + 10.982 *AA*(*I*)*m*), one based on twice as many cycles and having $r = 0.935$ and $se = 15.6$, one estimates *RM*(24) = 123 ± 28 (the 90% prediction interval), suggesting only a 5% chance that cycle 24's *RM* will be smaller than 95 or larger than 151. The weighted mean prediction for cycle 24's *RM* based on the 11 statistically important single-variate geomagnetic precursor fits is 116 ± 34. Even if one opts to use the late-peak geomagnetic values rather than the true peak values, the weighted mean prediction remains essentially the same: 118 ± 36.

Using the best bi-variate geomagnetic precursor fit (*RM* = –203.346 + 4.514 *APM*# + 26.344 *APm*#, where # means the maximum value is the post-(*E*(*RM*)) value and the minimum value is the minimum in the vicinity of cycle minimum), having $r = 0.981$ and $se = 8.157$, one estimates *RM*(24) = 92 ± 27 (the 90% prediction interval), suggesting only a 5% chance that cycle 24's *RM* will be smaller than 65 or larger than 119. The best bi-variate fit based on the *AA*(*I*) index and twice as many cycles predicts *RM*(24) = 138 ± 29 (the 90% prediction interval), suggesting only a 5% chance that cycle 24's *RM* will be smaller than 109 or larger than 167. The best bi-variate fit using late-peak values; i.e., *AA*(*I*)*M*(*lp*) and *AA*(*I*)*m**, predicts *RM*(24) = 123 ± 29 (the 90% prediction interval), suggesting only a 5% chance that cycle 24's *RM* will be smaller than 80 or larger than 152. The weighted mean prediction for cycle 24's *RM* based on 22 statistically important bi-variate geomagnetic precursor fits is 112 ± 32.

The late-cycle 23 geomagnetic and solar wind velocity behaviors bear little resemblance to the mean of cycles 20–23 near cycle minimum behavior, suggesting, perhaps, that cycle 24 might be a statistical outlier. If not, then cycle 24 probably will be a smaller than average size cycle and minimums in the geomagnetic indices and the solar wind velocity have not yet occurred, but will be seen later in 2008–2009. Disregarding the off-sets, the late-cycle 23 *AA* and *AA*(*I*) behaviors appear more reminiscent of cycle 14's near cycle minimum behavior than the mean of cycles 20–23 near cycle minimum behavior, cycle 14 being the smallest cycle in the modern record (64.2).

Because of a lack of consensus, the NOAA Solar Cycle 24 Prediction Panel[14] issued two disparate predictions for the size of cycle 24: 140 ± 20 (the high prediction), peaking in late 2011, and 90 ± 10 (the low prediction), peaking in mid 2012. As the present study has shown, dependent upon which comparative geomagnetic precursor parameter is used, both the high and low predictions appear valid. So, it is with great anticipation that solar researchers eagerly await the unfolding of cycle 24. Will it be a fast riser of larger than average maximum amplitude or a slow riser of smaller than average maximum amplitude? Will it persist shorter than the average 11-yr length or follow that of cycle 23 and be of longer duration? Does another Maunder-like minimum lie ahead soon for the Sun or does it still lie well into the future? Are polar fields the better predictor of solar activity or is there something else available that will be revealed to improve solar activity prediction? Is there a dynamo model that really proves superior in accurately predicting the timing and sizes of solar activity? Many questions remain.

REFERENCES

1. Hathaway, D.H.; Wilson, R.M.; and Reichmann, E.J.: "A Survey and Synthesis of Solar Cycle Prediction Techniques," *J. Geophys. Res.*, Vol. 104, p. 22,375, 1999.

2. Kane, R.P.: "Did Predictions of the Maximum Sunspot Number for Cycle 23 Come True?" *Solar Phys.*, Vol. 202, p. 395, 2001.

3. Rangarajan, G.K.: "Sunspot Variability and An Attempt to Predict Solar Cycle 23 by Adaptive Filtering," *Earth, Planets, and Space*, Vol. 50, p. 91, 1998.

4. Kane, R.P.: "Prediction of the Sunspot Maximum of Solar Cycle 23 by Extrapolation of Spectral Components," *Solar Phys.*, Vol. 189, p. 217, 1999.

5. Li, K.J.; Yun, H.S.; and Gu, X.M.: "On Long-Term Predictions of the Maximum Sunspot Numbers of Solar Cycles 21 to 23," *Astron and Astrophys.*, Vol. 368, p. 285, 2001.

6. Schatten, K.H.; Scherrer, P.H.; Svalgaard, L.; and Wilcox, J.M.: "Using Dynamo Theory to Predict the Sunspot Number During Solar Cycle 21," *Geophys. Res. Letts.*, Vol. 5, p. 411, 1978.

7. Schatten, K.H.; and Hedin, A.E.: "A Dynamo Theory Prediction for Solar Cycle 22 – Sunspot Number, Radio Flux, Exospheric Temperature, and Total Density at 400 km," *Geophys. Res. Letts.*, Vol. 11, p. 873, 1984.

8. Schatten, K.H.; and Pesnell, W.D.: "An Early Solar Dynamo Prediction: Cycle 23 is Approximately Cycle 22," *Geophys. Res. Letts.*, Vol. 20, p. 2,275, 1993.

9. Pesnell, W.D.: "Predictions of Solar Cycle 24," *Solar Phys.*, Vol. 252, p. 209, 2008.

10. Harvey, K.L; and White, O.R.: "What is Solar Minimum?" *J. Geophys. Res.*, Vol. 104, p. 19,759, 1999.

11. Zhan, L.; Zhao, H.; and Liang, H.: "Prediction of Sunspot Numbers in the Declining Phase of Solar Cycle 23," *New Astronomy*, Vol. 8, p. 449, 2003.

12. Wilson, R.M.; and Hathaway, D.H.: "Anticipating Cycle 24 Minimum and Its Consequences: An Update," *NASA/TP—2008–215576*, Marshall Space Flight Center, AL, October 2008, <http://trs.nis.nasa.gov/archive/00000793/>.

13. Wilson, R.M.: and Hathaway, D.H.: "On the Period-Amplitude and Amplitude-Period Relationships," *NASA/TP—2008–215580*, Marshall Space Flight Center, AL, November 2008.

14. <ftp://ftp.ngdc.noaa.gov/STP/SOLAR_DATA/SUNSPOT_NUMBERS/>, Accessed 2008.

15. Svalgaard, L.; Cliver, E.W.; and Le Sager, P.: "IHV: A New Long-Term Geomagnetic Index," *Adv. Space Res.*, Vol. 34, p. 436, 2004.

16. Wilson, R.M.; and Hathaway, D.H.: "An Examination of Selected Geomagnetic Indices in Relation to the Sunspot Cycle," *NASA/TP—2006–214711*, Marshall Space Flight Center, AL, December 2006, <http://trs.nis.nasa.gov/archive/00000741/>.

17. Ohl, A.I.: *Solice Dann.*, No. 12, p. 84, 1966.

18. Ohl, A.I.: *Geomagnetizm i Aeronomiya*, Vol. 11, p. 549, 1971.

19. Feynman, J.: "Geomagnetic and Solar Wind Cycles, 1900–1975," *J. Geophys. Res.*, Vol. 87, p. 6,153, 1982.

20. Bravo, S.; and Otaola, J.A.: "Polar Coronal Holes and the Sunspot Cycle – A New Method to Predict Sunspot Numbers," *Solar Phys.*, Vol. 122, p. 335, 1989.

21. Thompson, R.J.: "A Technique for Predicting the Amplitude of the Solar Cycle," *Solar Phys.*, Vol. 148, p. 383, 1993.

22. Dabas, R.S.; Sharma, K.; Das, R.M.; et al.: "A Prediction of Solar Cycle 24 Using a Modified Precursor Method," *Solar Phys.*, Vol. 250, p. 171, 2008.

23. Wilson, R.M.; and Hathaway, D.H.: "Using the Modified Precursor Method to Estimate the Size of Cycle 24," *NASA/TP—2008–215467*, Marshall Space Flight Center, AL, July 2008.

24. Wilson, R.M.; and Hathaway, D.H.: "On the Relationship Between Solar Wind Speed, Earthward-Directed Coronal Mass Ejections, Geomagnetic Activity, and the Sunspot Cycle Using 12-Month Moving Averages," *NASA/TP—2008–215413*, Marshall Space Flight Center, AL, June 2008.

25. Coordinated Data Analysis Web, Goddard Space Flight Center, <http://cdaweb.gsfc.nasa.gov/>, Accessed 2008.

26. Wilson, R.M.; Hathaway, D.H.; and Reichmann, E.J.: "On the Importance of Cycle Minimum in Sunspot Cycle Prediction," *NASA/TP—1996–3648*, Marshall Space Flight Center, AL, August 1996, <http://trs.nis.nasa.gov/archive/00000335/>.

27. Ehrenberg, A.S.C.: *A Primer in Data Reduction*, John Wiley & Sons, New York, p. 200, 1982.

28. Solar Cycle 24 Prediction Issued April 2007, <http://www.swpc.noaa.gov/SolarCycle/SC24/index.html>, Accessed 2008.

29. Berger, A.; Goossens, C.; and Pestiaux, P.: "Predictability of the Wolf Sunspot Number," in *Solar-Terrestrial Predictions*: *Proceedings of a Workshop at Meudon, France, June 18–22, 1984*, P.A. Simon, G. Heckman, and M.A. Shea (Eds.), National Oceanic and Atmospheric Administration, Environmental Laboratory, Boulder, CO, Air Force Geophysics Laboratory, Bedford, MA, p. 13, 1986.

30. Gnevyshev, M.N.; and Ohl, A.I.: "On the 22-Year Solar Activity Cycle," *Astron. Z.*, Vol. 25, p. 18, 1948.

31. Vitinskii, Y.I.: "Solar Activity Forecasting," *NASA/TTF–1965–289*, Washington, DC, 1965.

32. Schatten, K.H.: "Solar Activity Prediction: Timing Predictors and Cycle 24," *J. Geophys. Res.*, Vol. 107, p. SSH15-1, 2002.

33. Wang, J.-L.; Gong, J.-C.; Liu, S.-Q.; et al.: "The Prediction of Maximum Amplitudes of Solar Cycles and the Maximum Amplitude of Solar Cycle 24," *Chin. J. Astron. & Astrophys.*, Vol. 2, p. 557, 2002.

34. Duhau, S.: "An Early Prediction of Maximum Sunspot Number in Solar Cycle 24," *Solar Phys.*, Vol. 213, p. 203, 2003.

35. Sello, S.: "Solar Cycle Activity: A Preliminary Prediction for Cycle #24," *Astron and Astrophys.*, Vol. 410, p. 691, 2003.

36. Hathaway, D.H.; Nandy, D.; Wilson, R.M.; and Reichmann, E.J.: "Evidence that a Deep Meridional Flow Sets the Sunspot Cycle Period," *Astrophys. J.*, Vol. 589, p. 665, 2003.

37. Hathaway, D.H.; Nandy, D.; Wilson, R.M.; and Reichmann, E.J.: "Erratum: 'Evidence that a Deep Meridional Flow Sets the Sunspot Cycle Period' (ApJ, 589, 665 [2003])," *Astrophys. J.*, Vol. 602, p. 543, 2004.

38. Svalgaard, L.; Cliver, E.W.; and Kamide, Y.: "Sunspot Cycle 24: Smallest Cycle in 100 Years?" *Geophys. Res. Letts.*, Vol. 32, p. L01104, 2005.

39. Jain, R.: "Prediction of the Amplitude in Sunspot Cycle 24," Paper Presented 36th COSPAR Scientific Assembly Held July 16–23, 2006, in Beijing, China, Meeting Abstract from CD–ROM No. 642, 2006.

40. Dikpati, M.; de Toma, G.; and Gilman, P.A.: "Predicting the Strength of Solar Cycle 24 Using a Flux-Transport Dynamo-Based Tool," *Geophys. Res. Letts.*, Vol. 33, p. L05102, 2006.

41. Hathaway, D.H.; and Wilson, R.M.: "Geomagnetic Activity Indicates Large Amplitude for Cycle 24," *Geophys. Res. Letts.*, Vol. 33, p. L18101, 2006.

42. Choudhuri, A.R.; Chatterjee, P.; and Jiang, J.: “Predicting Solar Cycle 24 with a Solar Dynamo Model,” *Phys. Rev. Letts.*, Vol. 98, p. 131,103, 2007.

43. Obridko, V.N.; and Shelting, B.D.: “On Prediction of the Strength of the 11-Year Solar Cycle No. 24,” *Solar Phys.*, Vol. 248, p. 191, 2008.

44. Hiremath, K.M.: “Prediction of Solar Cycle 24 and Beyond,” *Astrophys. and Space Science*, Vol. 314, p. 45, 2008.

45. Javaraiah, J.: “North-South Asymmetry in Solar Activity: Predicting the Amplitude of the Next Solar Cycle,” *MNRAS*, Vol. 377, p. L34, 2007.

46. Javaraiah, J.: “Predicting the Amplitude of a Solar Cycle Using the North-South Asymmetry in the Previous Cycle: II. An Improved Prediction for Solar Cycle 24,” *Solar Phys.*, Vol. 252, Issue 2, pp. 419–439, 2008.

REPORT DOCUMENTATION PAGE					Form Approved OMB No. 0704-0188

1. REPORT DATE *(DD-MM-YYYY)* 01–02–2009	**2. REPORT TYPE** Technical Publication	**3. DATES COVERED** *(From - To)*
4. TITLE AND SUBTITLE Predicting the Size of Sunspot Cycle 24 on the Basis of Single- and Bi-Variate Geomagnetic Precursor Methods		**5a. CONTRACT NUMBER** **5b. GRANT NUMBER** **5c. PROGRAM ELEMENT NUMBER**
6. AUTHOR(S) Robert M. Wilson and David H. Hathaway		**5d. PROJECT NUMBER** **5e. TASK NUMBER** **5f. WORK UNIT NUMBER**
7. PERFORMING ORGANIZATION NAME(S) AND ADDRESS(ES) George C. Marshall Space Flight Center Marshall Space Flight Center, AL 35812		**8. PERFORMING ORGANIZATION REPORT NUMBER** M–1250
9. SPONSORING/MONITORING AGENCY NAME(S) AND ADDRESS(ES) National Aeronautics and Space Administration Washington, DC 20546–0001		**10. SPONSORING/MONITOR'S ACRONYM(S)** NASA **11. SPONSORING/MONITORING REPORT NUMBER** NASA/TP—2009–215687

12. DISTRIBUTION/AVAILABILITY STATEMENT
Unclassified-Unlimited
Subject Category 92
Availability: NASA CASI (443–757–5802)

13. SUPPLEMENTARY NOTES
Prepared by the Science and Exploration Vehicle Office, Science and Mission Systems Office

14. ABSTRACT
Examined are single- and bi-variate geomagnetic precursors for predicting the maximum amplitude (*RM*) of a sunspot cycle several years in advance. The best single-variate fit is one based on the average of the *ap* index 36 mo prior to cycle minimum occurrence (*E*(*Rm*)), having a coefficient of correlation (*r*) equal to 0.97 and a standard error of estimate (*se*) equal to 9.3. Presuming cycle 24 not to be a statistical outlier and its minimum in March 2008, the fit suggests cycle 24's *RM* to be about 69 ± 20 (the 90% prediction interval). The weighted mean prediction of 11 statistically important single-variate fits is 116 ± 34. The best bi-variate fit is one based on the maximum and minimum values of the 12-mma of the *ap* index; i.e., *APM*# and *APm**, where # means the value post-*E*(*RM*) for the preceding cycle and * means the value in the vicinity of cycle minimum, having $r = 0.98$ and $se = 8.2$. It predicts cycle 24's *RM* to be about 92 ± 27. The weighted mean prediction of 22 statistically important bi-variate fits is 112 ± 32. Thus, cycle 24's *RM* is expected to lie somewhere within the range of about 82 to 144. Also examined are the late-cycle 23 behaviors of geomagnetic indices and solar wind velocity in comparison to the mean behaviors of cycles 20–23 and the geomagnetic indices of cycle 14 ($RM = 64.2$), the weakest sunspot cycle of the modern era.

15. SUBJECT TERMS
Sun, sunspot cycle, solar activity, precursor methods, solar cycle prediction, cycle 24

16. SECURITY CLASSIFICATION OF:			**17. LIMITATION OF ABSTRACT**	**18. NUMBER OF PAGES**	**19a. NAME OF RESPONSIBLE PERSON**
a. REPORT	**b. ABSTRACT**	**c. THIS PAGE**			STI Help Desk at email: help@sti.nasa.gov
U	U	U	UU	40	**19b. TELEPHONE NUMBER** *(Include area code)* STI Help Desk at: 443-757-5802

National Aeronautics and
Space Administration
IS20
George C. Marshall Space Flight Center
Marshall Space Flight Center, Alabama
35812